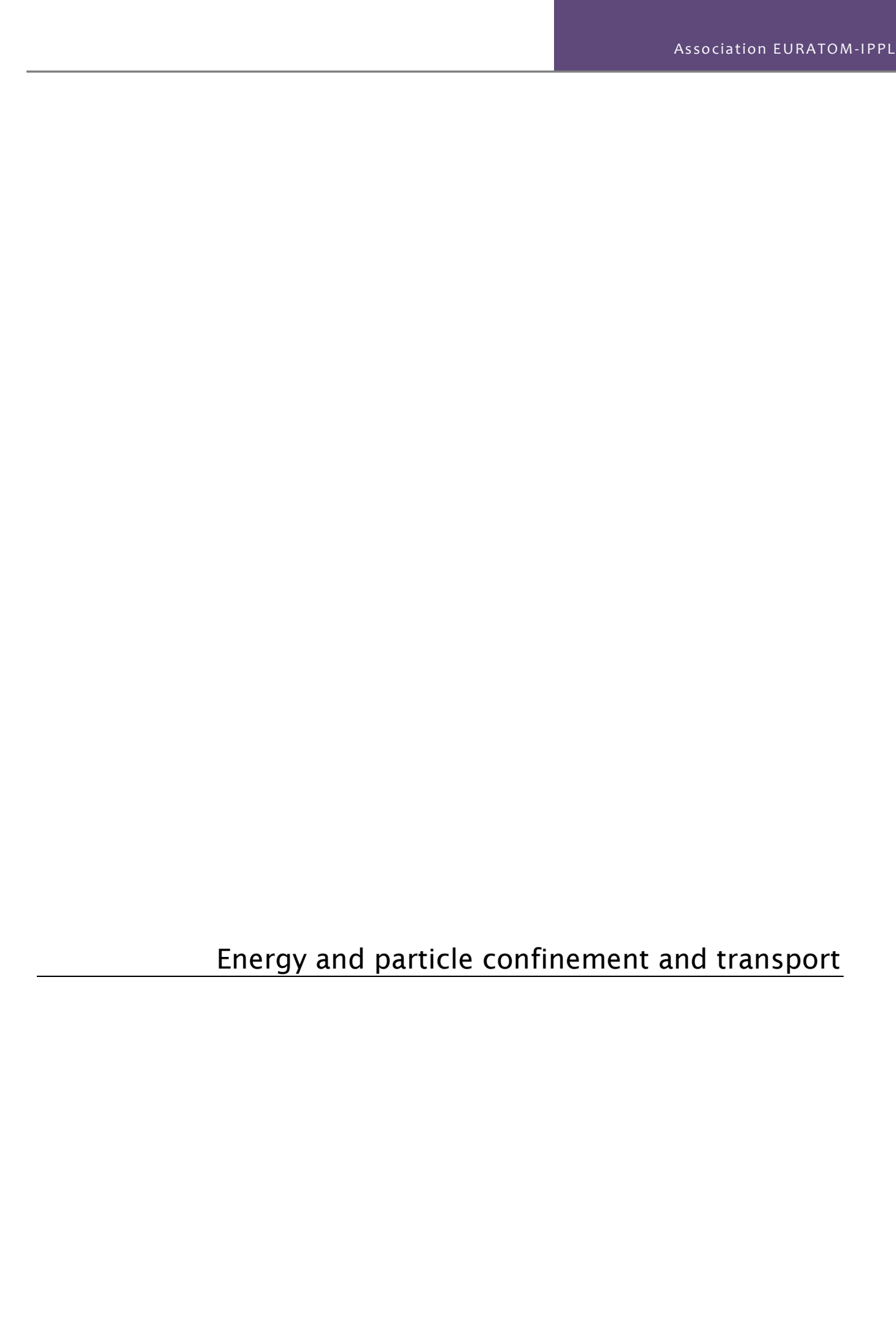
#### 2 Fusion Plasma Physics

Work in fusion plasma physics includes 13 tasks. The tasks are grouped under the four following subheadings:

- Energy and particle confinement and transport
  - Tokamak modelling
  - Studies of material erosion and re-deposition on plasma-facing components from the TEXTOR tokamak
- Energetic particle physics
  - o Čerenkov detectors for fast electron measurements: new diagnostics for Tore-Supra
  - o Development and application of neutron diagnostics for magnetic confinement devices
  - Applications of solid-state nuclear track detectors (SSNTDs) for fast ion and fusion reaction product measurements in TEXTOR experiments
- Fusion plasma diagnostics
  - Spectrometry of soft X-ray emission from W7-X stellarator by the use of fast counting semiconductor detectors
  - o C-, O- monitor system for W7-X
  - o Microwave diagnostic development
  - Detection of the delayed neutrons from activation of fissionable materials in the neutron field at fusion-plasma devices
- Theory and modeling for improved concepts and for ITER
  - Nonlinear dynamics of fast ion driven plasma modes near instability threshold theoretical basis for integrated tokamak modelling
  - Stochastic processes and stochastic representations for the kinetic equations of a gas of charged particles
- Inertial fusion energy "keep-in-touch" activity
  - o Studies on fast ignition of inertial fusion using laser-driven proton beams
  - o Formation of plasma jets and their interaction with ambient media



### 2.1 Tokamak modeling

Roman Stankiewicz and Sebastian Głowacz Institute of Plasma Physics and Laser Microfusion romsta@ifpilm.waw.pl

#### **Abstract**

The numerical studies of plasma performance in fusion reactors (ITER, DEMO), JET discharges and contribution to the development of modular transport code by participating in the TF-ITM Project 3 are presented.

#### Summary

The impurity radiation, allowing for the reduction of the power loads to target plate below a level that would be sustainable for the plate material, is essential for future reactor operation. The code COREDIV has been used to perform numerical studies of steady state operation for tungsten as sputtered impurity and for argon as seeded impurity. The codes COREDIV, EDGE2D/EIRENE have been also used to analyzed the present and future JET experiments with ITER like wall and advanced scenario.

The effort to developed modular system of codes, modeling various physical processes, has been undertaken in TF-ITM project 3. The participation in TF-ITM Project 3 in developing ETS ( European Transport Solver ) is also present in this report.

### Computation of Radiative Energy Exhaust by Sputtered and Seeded Impurities in Fusion Reactors with Tungsten Wall

The numerical analysis of the line radiation losses in ITER, DEMO A and DEMO D has been performed using the code COREDIV, previously used to model the regimes of ITER reactor for carbon, nickel and molybdenum as sputtered impurity [1] In the presented analysis the tungsten as sputtered impurity and argon as seeded impurity is considered.

The sputtering of tungsten includes contributions from all ions interacting with divertor plates. The code COREDIV solves in self-inconsistent way the core and boundary region. The description of the model used in COREDIV can be found in [1]. The scan with respect of Ar source intensity has been performed. The table demonstrate the possibility of the reduction of power load o the divertor plate.

#### Analysis of JET discharges

In JET ELMy H mode discharges with carbon plate and seeded impurities (N,NE) the 95% of power is radiated leading to the detachment of both divertor legs and reduction of size of of ELMs by a factor of 10. The above discharges have been modeled using the EDGE2D/EIRENE plasma fluid/Monte-Carlo neutral code package. The ELMs has been modeled by intermittently destroying the transport barrier, i.e. increasing the transport across separatrix. The results of simulation has been presented in [2].

The analysis of future JET discharges with all-metal wall and advanced scenarios has been presented in [3]. Such a discharges will be characterized by relatively low density and high power both necessary to induced high bootstrap current. Since the energy balance depends strongly on the coupling between the bulk plasma and the SOL and divertor region the code COREDIV, solving self-consistently transport in both region, can be used to analyze such discharges. In order to fix some code parameter. JET discharges characterized by low density, high triangularity and different radiation level has been compare with code results. The scan of the heat load dependence on the position of X point with respect to target plate and density of seeded impurity (N,Ne).

reactor	heating power	power to plate
	MW	MW
DEMO A	1100	93
DEMO D	430	21
ITER	109	31

#### Participation in TF-ITM Project 3

In the frame of TF-ITM project we cooperate in developments of ETS (European Transport Solver). It was assumed that ETS will solve the 1D time evolution equations for poloidal flux, ions densities, temperatures and toroidal velocities [4]. In IFPILM one of the numerical method, based on finite difference approximation and coded. The method of manufactured solution was used to calculate the source terms of the equations from the assumed profiles for the solution, transport coefficient and metric coefficients. The main advantage of using this procedure is the possibility to compare the solution of the system of nonlinear coupled equation with the exact one. The check of coding the general form of ETS and the performance of numerical procedures has been done. The module for impurity solving the transport equations for impurity densities has been also developed.

The presented work can be divided into two parts:

- a)The analysis of the of Jet discharges and future reactors was focused on the possibility of using added and sputtered impurities to reduce the power load to divertor plates below a level that would be sustainable for the plate material. The results shows that it possible for some combination of impurities.
- b) The participation in ITM project consist of :preparation of manufactured method of analytic solution allowing for testing ETS (European Transport Solver), implementation of the numerical scheme based on central finite difference approximation, development of the modules for impurities, participation in developing the whole structure of ETS.

#### Conclusions

The results shows that sufficiently large part of power can be radiated by impurity. However it should be stressed that this results has been obtained under some simplification of physical model used in COREDIV. The weak point of the presented model is the lack of good anomalous transport description for both main and impurity ions. The development of Analytics module allows for extensive testing of ETS.

#### Collaboration

Association EURATOM – IPP, Garching, Germany Association EURATOM – FZJ, Institute of Plasma Physics, Juelich, Germany Association EURATOM – UKAEA Culham Science Center, Abingdon, UK

- [1] G.Telesca et al., Nucl.Fusion 47 (2007) 1625
- [2] D. Moulton, W. Fundamentski, S. Wiesen, S. Głowacz, R. Zagorski and JET EFDA contributors, *EDGE2D/EIRENE simulation of seeded ELMY H-mode discharges on JET*, 19th PSI Conference, submitted to J.Nuclear Materials.
- [3] R. Zagórski, G.Telesca, G. Arnoud, W. Fundamentski, G. Giroud, S. Głowacz, S. Joachimek, K. McCormick and JET EFDA contributors, *Selfconsistent modeling of impurity seeded JET advanced scenarios*, 19th PSI Conference, submitted to J.Nuclear Materials.
- [4] D. Kalupin, J. F.Artaud, D. Coster, S. Głowacz, S. Moradi, G. Perevezev, R. Stankiewicz, M. Tokar, at al., *Const ruction of European Transport Solver under the European Integrating Modeling Task Force*. EPS Conference 2008

## 2.2 Studies of material erosion and re-deposition on plasma facing components from the TEXTOR tokamak

Elżbieta Fortuna-Zaleśna Warsaw University of Technology, Materials Science and Engineering Faculty elaf@inmat.pw.edu.pl

Joanna Zdunek, Witold Zieliński, Mariusz Andrzejczuk, Marcin Pisarek, Tomasz Płociński, Stanisław Szpilewicz, Marcin Rasiński, and Krzysztof J. Kurzydłowski

#### **Abstract**

Studies of the microstructure and chemical composition of the plasma facing components originating from the TEXTOR and ASDEX-Upgrade tokamaks were carried out to improve understanding of the mechanism of material erosion and re-deposition. The following tasks were undertaken:

- 1. characterization of the plasma-induced damage in high Z metals used as limiters,
- 2. characterization of material mixing occurring in high Z metals used as limiters,
- 3. characterization of the co-deposits.

#### Summary

Studies of the microstructure and chemical composition of the plasma facing components originating from the TEXTOR and ASDEX-Upgrade (AUG) tokamaks were carried out to improve the understanding of the mechanisms of material erosion and re-deposition. In particular, the following tasks were performed:

- 1. Post mortem analysis of tungsten coated tiles from the divertor strike point region of AUG and
- 2. Dust examinations (originating from TEXTOR and AUG).

#### Ad 1.

The investigation concerned 9 samples from two divertor strikepoint tiles of ASDEX Upgrade, designated as Element 01b/1 and Element 04/1. The tiles were installed from 4/07 to 10/07. During this campaign all PFCs were tungsten coated and no boronization was performed. The tile denoted as Element 01b/1, which came from the outer strikepoint region, was coated with a 200 $\mu$ m W VPS layer. The tile Element 04/1, from the inner strikepoint region, was coated with a 4  $\mu$ m W PVD layer.

The aim of these post-mortem examinations (SEM, EDS, TEM, HRTEM, FIB, XPS, AES, GI-XRD) was material mixing and plasma-induced damage of tungsten coatings.

It has been generally observed that the coating morphology was modified by high-heat loads and co-deposition of species from plasma. SEM observations of the inner divertor strike point tile revealed the presence of a thick, compact, glassy-like deposit with good adhesion and integrity. Areas with remelted layer of tungsten were observed. In the case of outer strike point region the observations revealed large surface areas subjected to erosion.

The XPS examinations revealed that the main constituents of the deposits are carbon (35 at. %), tungsten (35 at.%) and oxygen (28 at.%). Nitrogen and iron was present at the level of 1at. % (inner divertor strike point tile).

TEM examinations revealed stratified structure of thick deposit (up to  $1.5 \mu m$  thick). The observed sublayers differ in thickness (10-50 nm), structure and chemical composition. The diffraction patterns prove their amorphous character (inner divertor strike point tile).

The GI-XRD studies showed the major phase identified is metallic tungsten. One can not, however, exclude the presence of small amount of tungsten carbides and graphite.

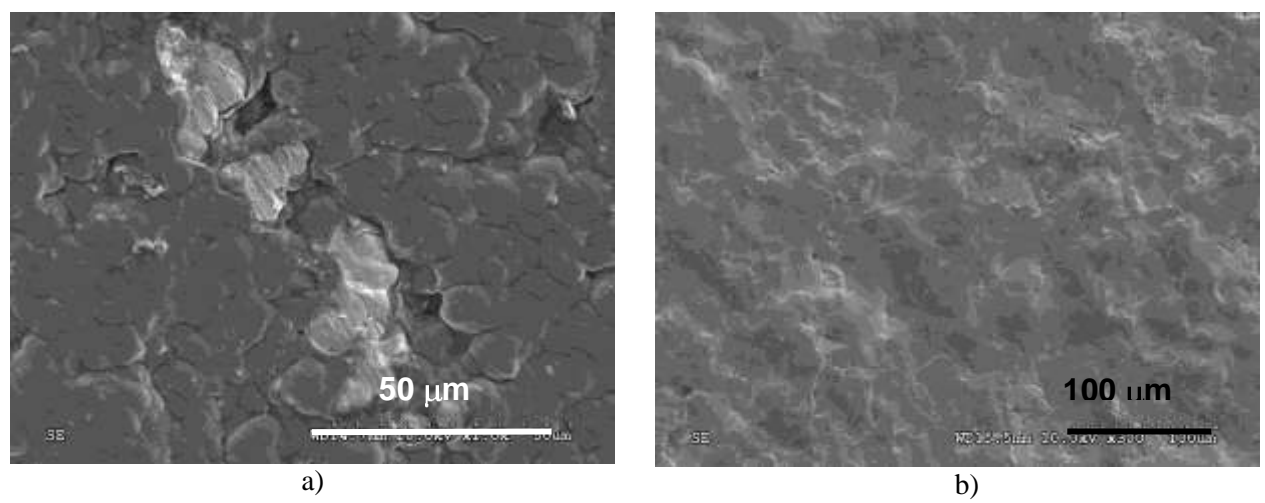


Figure 1. SEM images of the Element 04/1 (a) and Element 01/b (b) tiles surface

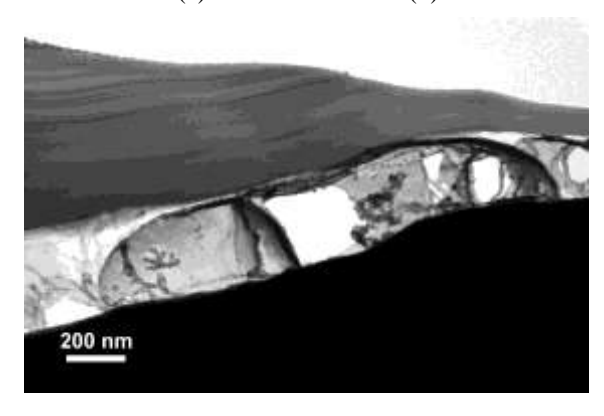


Figure 2. TEM images of deposit at the surface of tungsten coating

#### Ad. 2.

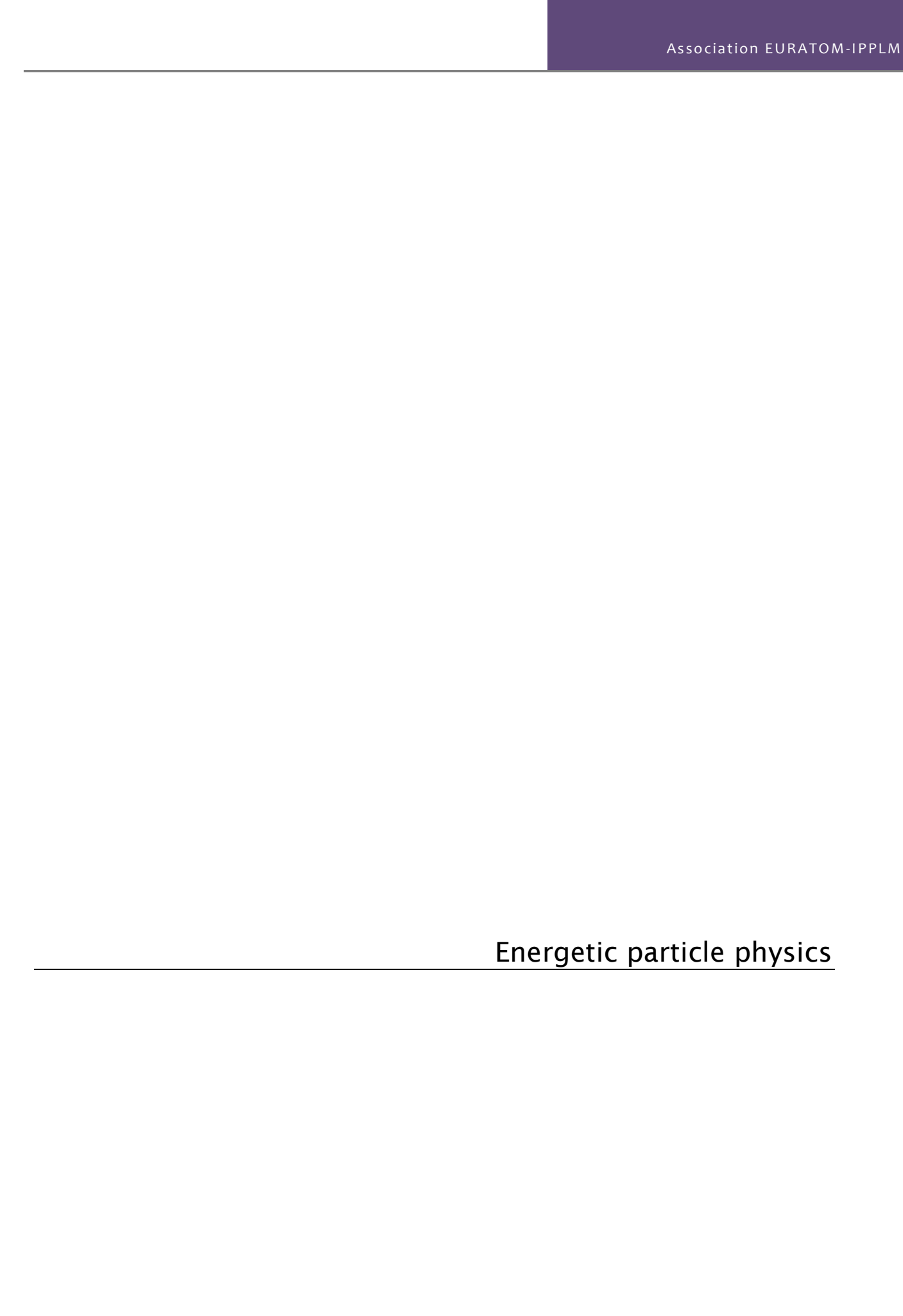
The BET surface of dust samples collected in TEXTOR (neutralizer plate) were measured using the QuadraSorb SI by Quantachrome Instruments. Before measurement the samples were outgassing at 300oC for 3 hours. The analysis was conducted in nitrogen at 77.3 K. The measured surface area was 24.22 m<sup>2</sup>/g.

At the end of 2008, the examinations of dust probes collected in AUG in May 2005 and November 2007 started. The samples were all taken from stainless steel parts using the adhesive strip technique (6 different locations). The examinations include observations of dust particles size and morphologies and measurements of chemical composition using SEM, HRESEM, FIB and TEM techniques.

#### Collaboration

Association EURATOM - IPP, Garching, Germany

- [1] NIST XPS database http://srdata.nist.gov/xps/
- [2] www.lasurface.com/database/elementxps.php
- [3] Handbook of X-ray Photoelectron Spectroscopy by J. F. Moulder, W.F. Stickle, P. E. Sobol and K. D. Bomben, published by ULVAC-PHI. Inc.



# 2.3 Čerenkov detectors for fast electron measurements: new diagnostics for Tore-Supra

Lech Jakubowski
The Andrzej Soltan Institute for Nuclear Studies
Lech.Jakubowski@ipj.gov.pl

Karol Malinowski, Marek Rabiński, Marek J. Sadowski, Jarosław Żebrowski, Krzysztof Czaus, Marcin Jakubowski, Robert Mirowski, Paweł Karpiński, and Andrzej Wiraszka

#### **Abstract**

The significant progress in the design and manufacturing of an appropriate Cherenkov-type detector dedicated to measurements of fast electron beams within the edge region of the Tore-Supra facility at CEA-Cadarache, which was achieved by the IPJ team in the previous years, made possible to perform the first preliminary electron beams measurements within Tore-Supra in 2008. The analysis of the preliminary experiment within the ISTTOK facility in Lisbon, which was realized by means of the simply, single-channel detector, was also performed and the obtained results were published. A new four-channel measuring head, which was assigned for electron measurements at relatively low thermal loads inside the ISTTOK, was designed and manufactured. Results of the last experimental campaign, as performed with the application of another simple detector within the CASTOR device in Prague, have been finally published.

#### Summary

In 2008 research on design and applications of Cherenkov-type detectors for measurements of fast electrons in tokamak-type facilities were concentrated on two main tasks (concerning Tore-Supra and ISTTOK) and on one supplementary task (concerning CASTOR):

- a) The completion of the manufacturing of the new Cherenkov-detector prototype, designed especially for studies of supra-thermal electrons within Tore-Supra technical, and the realization of preliminary electron beams measurements during the November 2008 experimental campaign;
- b) The analysis of results from measurements during the preliminary 2007 experimental session (presented in three papers), as well as the manufacturing and preparation of the new four-channel Cherenkov detector head designed especially for measurements within ISTTOK;
- c) Analysis of experimental results obtained within CASTOR device in 2006, which were finally published in two papers in the first quarter of 2008 [4-5].

Ad a). In 2008 the Cherenkov detector measuring head – which was designed especially for plasma conditions occurring in a scrape-of-layer (SOL) within the Tore-Supra tokamak (at CEA in Cadarache) – was finally manufactured and tested at IPJ. The four-channel Cherenkov detector measuring head, which was mounted on the top of the new reciprocating shaft, was inserted into the Tore Supra tokamak chamber in November 2008. Successive channels, counted from the top of the probe, were equipped with diamond radiators shielded with Molybdenum foil-filters of different thickness (100  $\mu m$ , 50  $\mu m$ , 20  $\mu m$  and 10  $\mu m$ ). They enabled to record the fast electrons beams with following minimum energies: Ee4 > 259 keV, Ee3 > 173 keV, Ee2 > 109 keV and Ee1 > 84 keV. The internal shaft was located in one of the vertical diagnostic ports and it enabled the measuring head to be moved into the SOL region along the tokamak small radius – always outside the Last Close Flux Surface (LCFS) – to the nearest positions, in which the top of the measuring head was placed 80-100 mm from the LCFS.

Signals from four channels of detector were recorded for about 140 shots performed during the last 2008 experimental campaign. Visible light generated by the Cherenkov-effect was detected outside the Tore-Supra hall by means of four separate photomultipliers. The background level of the signals from four

photomultipliers was low, but there appeared some spikes at the level of hundreds mV. The averaged Cherenkov detector signals were recorded on the 10 mV level. Therefore, for the recording of Cherenkov signals, we had to use a fast digital oscilloscope. Finally, for the three last shots of the campaign, the scope time base was chosen to be 200 ms, with the sampling time equal to  $0.2~\mu s$  and for two last Tore-Supra shots the measuring head was moved into the close vicinity of the LCFS two times per each shot.

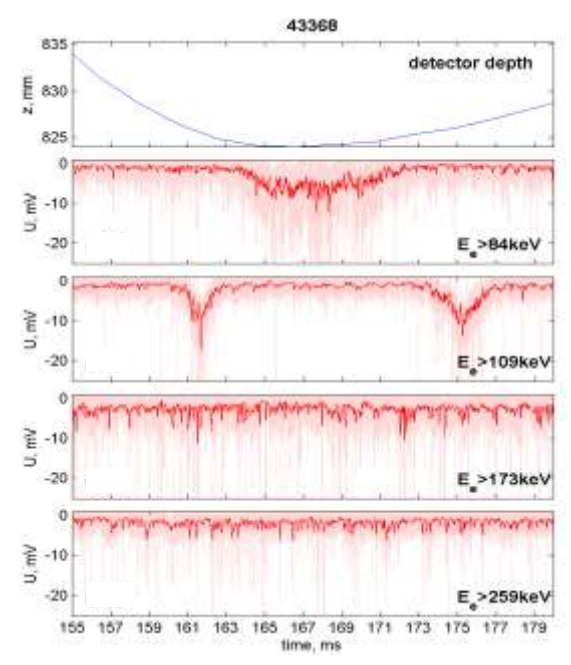


**Figure 1** Set of signals from different channels of the Cherenkov detector (four lower traces) and the detector vertical position (the upper trace), as recorded for TS43368 shot (start point of the time scale corresponded to t = 4.155 s).

There were recorded 6 sets of signals, corresponding to shots performed with an additional lower hybrid (LH) heating. The Cherenkov-produced signals were observed in two channels (for electron energy above 84 keV, and above 109 keV). The obtained signals were routinely correlated with the inner shaft movement (DENEPR) and other basic Tore-Supra plasma signals: i.e. LH heating, ICRH heating, plasma current (Ip), and the line-averaged plasma density (nl). It seems that the appearance of the Cherenkov signals, produced by about 150-keV fast-electron beams, was strongly dependent on sufficiently high level of the LH (and ICRH) heating. An example of the recorded Cherenkov signals for the case, when the measuring head was pushed into the LCFS vicinity not very deeply, is presented in Fig. 1.

The most important result was the statement that the recorded electron signals confirm the appearance of a thin fast-electron sheath outside the plasma torus in the Tore-Supra. That electron sheath appeared to be almost quasi-stationary in space during the movement of the Cherenkov detector head. The obtained results need further analysis and particular scrupulosity in their consideration, because there is a significant discrepancy between the measurements of Cherenkov detector and Langmuir probe diagnostics.

Ad b). In 2008 the IPJ team was involved in the elaboration of results obtained during the preliminary measurements, which were performed within the ISTTOK facility during several experimental sessions in 2007. The Cherenkov signals, which were recorded by means of a single channel Cherenkov detector head were analyzed and presented in three different papers [1-3]. In the papers the obtained experimental data were compared with results of numerical simulations. The most important result was the identification of operational regimes in the low-current ISTTOK discharges, when the fast run-away electrons are generated. The collected experimental data appeared to be in good agreement with results obtained previously by the numerical analysis of macroscopic plasma parameters. The new four-channel Cherenkov detector designed especially for measurements within ISTTOK was manufactured and finally tested by the IPJ team in 2008 also.

Ad c). Analysis of experimental results from CASTOR device was presented in two papers [4, 5].

#### Conclusions

It can be concluded that the most important achievement of Task P3 in 2008 was the preliminary electron beams measurements by means of the Cherenkov-type detector within Tore-Supra facility.

The P3 2008 milestone, planned in the collaboration with the Association EURATOM-CEA, was almost fully realized. The prototype Cherenkov-type detector was successfully applied for ripple-born electron measurements at a scrape-of-layer within of Tore-Supra tokamak. Some data were collected. The elaboration and analysis of the obtained experimental data should be continued by partners from the both research centres in 2009. It seems that some modifications of the measuring head construction are needed to get more reliable results. The members of the IPJ and CEA teams expect that the project will be continued in 2009.

The P3 2008 milestone, planned in the collaboration with the Association EURATOM-IST, was also almost fully realized. The elaboration of the preliminary experimental results was performed [1-3]. The new four-channel Cherenkov detector designed especially for ISTTOK plasma conditions was manufactured. The first measurements session has been shifted until 2009 first quarter, according to suggestion of our foreign partners.

It can be finally concluded that research on design and application of Cherenkov-type detectors of fast (ripple-born and runaway) electrons should be continued in order to elaborate appropriate detection systems for other experiments (e.g. ASDEX, JET) and future ITER.

#### Collaboration

Association EURATOM – CEA, Cadarache, France Association EURATOM – IST, Lisbon, Portugal

- [1] V.V. Plyusnin, L. Jakubowski, J. Żebrowski, H. Fernandes, C. Silva, P. Duarte, K. Malinowski, M. Rabiński, M.J. Sadowski, 35th EPS Conference on Plasma Phys. Hersonissos, 9 13 June 2008 ECA Vol.32, P-5.075 (2008).
- [2] V.V. Plyusnin, L. Jakubowski, J. Żebrowski, H. Fernandes, C. Silva, K. Malinowski, P. Duarte, M. Rabiński, M.J. Sadowski, Rev. Sci. Instrum. Vol. 79 (2008) 10F505.
- [3] C. Silva, H. Fernandes, C.A.F. Varandas, D. Alves, B.B. Carvalho, I. Carvalho, P. Carvalho, P.A. Carvalho, R. Coelho, A. Duarte, P. Duarte, H. Figueiredo, J. Figueiredo, J. Fortunato, R. Gomes, B. Goncalves, I. Nedzelskij, A. Neto, T. Pereira, V. Plyusnin, D. Valcárcel, P. Balan, C. Ionita, R. Schrittwieser, J.B. Correia, V. Livramento, O. Lielausis, A. Klyukin, E. Platacis, A. Sharakovski, I. Tale, T. Lunt, M. Gryaznevich, G. Van Oost, M. Hron, A. Malaquias, N. Dreval, A. Melnikov, P. Khorshid, C. R Gutierrez Tapia, W. Sa, M. Kolokoldarov, A. Czarnecka, L. Jakubowski, J. Żebrowski, K. Malinowski, M.J. Sadowski, Proc. 22nd IAEA Fusion Energy Conference, Geneva, October 13-18, 2008 ex\_p4-11 (2008).
- [4] J. Żebrowski, L. Jakubowski, M.J. Sadowski, K. Malinowski, M. Jakubowski, V. Weinzettl, J. Stockel, M. Vacha, M. Peterka, Proc. Intern. Conf. PLASMA-2007, Greifswald, Germany, Oct. 16-19, 2007, AIP CP Vol. 993 (2008) 255-258.
- [5] L. Jakubowski, M.J. Sadowski, J. Stanisławski, K. Malinowski, J. Żebrowski, M. Jakubowski, V. Weinzettl, J. Stockel, M. Vacha, M. Peterka, Proc. 17th IAEA Technical Meeting on RUSFD, Lisbon, Portugal, Oct. 22-24, 2007, AIP CP Vol. 996 (2008) 219-223.

## 2.4 Development and application of neutron diagnostics based on activation method for magnetic confinement devices

Marek Scholz Institute of Plasma Physics and Laser Microfusion marek@ifpilm.waw.pl

Barbara Bieńkowska, Maryla Chernyshova, Sławomir Jednoróg, Lech Karpiński, Marian Paduch, Rafał Prokopowicz, and Adam Szydłowski

#### **Abstract**

This paper describes investigations of neutrons produced by PF-6 device operating in the Institute of Plasma Physics and Laser Microfusion, Warsaw, Poland. This kind of device can be dedicated to in-situ calibration of neutron diagnostics using on large Magnetic Confinement Fusion devices. Main parameters of neutron radiation have been measured by scintillation probe and by activation technique. Simultaneously, neutron transport calculations have been performed by Monte Carlo method. Finally, experimental measurements and numerical calculations have allowed to conclude that plasma focus devices can be useful pulse neutron sources for different applications.

#### Summary

The ability to accurately and precisely monitor the fusion power is essential for the mission of large Magnetic Confinement Fusion (MCF) machines. This can be achieved by using the neutron diagnostic systems. Mentioned systems should apply the technique that demonstrates the highest accuracy of neutron measurements, especially the total neutron yield. Thus, the absolute calibrations should be performed for a range of neutron intensities usual for large MCF devices.

One of the calibration methods for such systems includes putting a (point) neutron source into the vacuum vessel and moving it through a large number of positions so as to map out the response expected from extended plasma. Ideally, a 2.5 MeV neutron source should be used to simulate the response from deuterium plasma as well as 14 MeV source would be useful for diagnostic of tritium plasma respectively.

The neutron chamber has been tested with regard to its neutron generation parameters. Initial investigations have been carried out for several activation materials including Hf, In, Cd, Al and Au. Qualitative as well as quantitative analyses have been performed based on semiconductor detector system equipped with coaxial precalibrated detector. More than 15 nuclear reactions with different energy threshold have finally been found out among the detector material. A considerable effort has been devoted to perform Monte Carlo calculations of the neutron transport with MCNP version 5 code and MCNP5DATA cross section library. Then, main parameters of 2.5 MeV neutron radiation (absolute yields) have been investigated by both the numerical and activation method.

In order to investigate neutrons generated from PF-6 device 50 shots with frequency 0.08 Hz have been performed with the deuterium pressure of 22.6 hP and 4 kJ discharge energy level (the condenser bank has been charged up to a voltage of 17 kV) to activated Indium samples.

Samples have been irradiated during the two series of 50 shots. After that the samples have been measured by HPGe  $\gamma$ -spectrometer in well defined geometry. The activity has been calculated for the moment of irradiation end. Reaction rate has been calculated taking into account decay process during irradiation with assumption that neutron yield and energy distribution is identical in each shot. So, the number of nuclei activated in one shot  $N_1$  can be thus calculated from measured activity  $A_0$ :

Detected nuclides and reactions with activities at the moment of irradiation end  $A_0$  and calculated number of nuclei per shot  $N_1$  are presented in tables 1 and 2 for each series of shots.

**TABLE 1.** Results for first series of shots.

Reaction	$A_0[\mathrm{Bq}]$	$N_1$	Error
In-113(n,n')In-113m	$0.81 \pm 0.18$	$1.5 \cdot 10^2$	± 22%
$In-113(n,\gamma)In-114m$	$4.04 \pm 6.58$	$5.1 \cdot 10^5$	± 163%
In-115(n,n')In-115m	$7.68 \pm 0.46$	$3.7 \cdot 10^3$	± 6%
In-115(n,γ)In-116m	$6.32 \pm 0.31$	$6.3 \cdot 10^2$	± 5%

TARIF 3	Results for second	d series of shots
I A DI (P/ .).	RESULIS TOL SECONO	i series of shots.

TABLE 5. Results for second series of shots.			
Reaction	$A_0[\mathbf{Bq}]$	$N_1$	Error
In-113(n,γ)In-114m	$0.56 \pm 1.70$	$6.9 \cdot 10^4$	± 305%
In-115(n,n')In-115m	$5.25 \pm 0.43$	$2.5 \cdot 10^3$	$\pm$ 8%
In-115(n, $\gamma$ )In-116m	$5.25 \pm 0.40$	$5.3 \cdot 10^2$	$\pm$ 8%
In-115 $(n,\gamma)$ In-116n	$102 \pm 131$		

The MCNP5 Monte Carlo code with MCNP5DATA cross section library have been used to calculate the number of atoms produced as a result of  $(n,\gamma)$  capture and (n,n') excitation with the samples. Simulations have been performed assuming that neutrons are emitted from point isotropic source and have Gaussian fusion energy spectrum with average of 2.45 MeV and FWHM = 0.12 MeV.

The number of atoms produced in the sample have been calculated using track length estimation tally multiplied by the microscopic cross section of the particular reaction. The number of simulated histories has been  $4\cdot10^6$ . The estimated relative errors achieved for the calculated results are less than 1%. Results are presented in Tab. 3.

<b>TABLE 3.</b> Results of MCNP calculations.				
Reaction	2.4.1.1.1 Number of produced			
	atoms per source neutron			
(n,n')	1.21·10 <sup>-6</sup>			
(n,γ)	1.85·10 <sup>-5</sup>			

According to the calculations made for irradiation of indium samples by MCNP code and activation measurements the neutron yield per shot can be evaluated. This results can be summarized in the following table:

TABLE 4.				
Number of series of shots	Reacti on	N <sub>1</sub> [atoms/shot]	Y <sub>n</sub> [neutrons/shot]	Error
1	(n,n')	$3.85 \cdot 10^3$	3.19·10 <sup>9</sup>	± 6%
1	(n,γ)	5.11·10 <sup>5</sup>	$2.76 \cdot 10^{10}$	± 163%
2	(n,n')	$2.50 \cdot 10^3$	2.07·109	± 8%
2	(n,γ)	6.95·10 <sup>4</sup>	3.76·10 <sup>9</sup>	± 303%

#### Conclusions

Obtained results have allowed to formulate the following conclusions:

- 1. PF-6 operates regularly with comparable neutron yield in each shot.
- 2. Maximum plasma current value has been roughly estimated from measured dI/dt waveforms and it is about 250-300 kA. So, the evaluated neutron yield from scaling law  $Y_n \sim 10^{-13} (I_{pmax})^4$  is lower than  $10^9$ .
- 3. The difference between measured and calculated from scaling law neutron yield can be provoked by a rough estimation of MCNP calculated number of produced atoms per source neutron as a results of used total cross section for Indium in the calculation.
- 4. Experimental results achieved from PF-6 device by means of activation technique confirmed that plasma-focus devices can be useful pulse neutron sources as a calibration source esspecially for 14 MeV neutrons.

## 2.5 Applications of solid-state nuclear detectors (SSNDTs) for fast ion and fusion reaction product measurements in TEXTOR experiments

Adam Szydłowski
The Andrzej Soltan Institute for Nuclear Studies
szydlowski@ipj.gov.pl

Aneta Malinowska, Karol Malinowski, Marek Rabiński, Marek J. Sadowski, Andrzej Gałkowski<sup>1</sup>, Mirosław Kuk, and Robert Mirowski

#### **Abstract**

Fast neutrons are in principle the only fusion reaction products which have been investigated extensively from the very beginning of fusion research. In fact, also fast protons and other electrically charged fusion reaction products (e.g. T, <sup>3</sup>He-, and <sup>4</sup>He-ions, 15-MeV protons etc.), carry away valuable information on plasma parameters and nuclear reaction mechanisms, and could be readily measured. However, to perform such a measurement a suitable detector is needed which could be located inside the experimental vessel and which could be operated under harsh plasma discharge conditions (such as high vacuum, high temperature, intense electromagnetic radiation, strong E-M interferences, etc.). Modern solid–state nuclear track detectors (NTD) appeared to be appropriate to withstand such conditions and have already been used in TEXTOR experiments. The first experimental results have shown that it is possible to discern craters produced in the detector by fusion reaction protons from other craters, and to convert the obtained pith dimension histograms into proton energy spectra. This report describes further investigations of energetic protons as well as low energy ions which were performed within the TEXTOR facility by means of NTD.

### Summary

In 2008 research on applications of solid-state nuclear detectors (SSNDTs) for fast ion and fusion reaction product measurements in TEXTOR experiments continued the previous measurements [4, 5]. A small ion-pinhole camera equipped with a PM-355 detector sample was placed below the plasma ring in the direction of ion drifts, at a distance of 4.4 cm from LCFS. However, in the described experiment it was aligned at an angle to the mayor TEXTOR radius, so that the input pinhole was oriented first at  $\gamma = 45^{\circ}$  (shots 108799 – 108818) and then  $\gamma = 60^{\circ}$  (shots 108832 – 108847). The plasma was heated in these discharges by one neutral beam (0.6 – 1.0 MW) only, and in the first series by ICRH at frequency of 38 MHz. The detector samples irradiated with fusion reaction protons which were emitted from these two series of shots were subject to the same interrupted etching procedure as the samples used in the calibration measurements [1, 2].

The detector sample which was irradiated in the first series of shots was etched only for 2 hours and scanned after that. Taking into account that the craters induced by fast protons could not be revealed after such short etching time [2] the craters observed on this sample were probably induced by other ions. One can suppose that the smaller diameter craters, those in a range of  $0.75-2~\mu m$ , were induced by fusion reaction tritons, whereas the larger etch pitches (from the range  $2-4~\mu m$ ) were produced by fast primary ions. In Fig. 1 there are presented two–dimensional distributions of craters in different diameter ranges, as were measured upon this sample. One can see that craters induced by lower energy ions are concentrated in a narrow area, whereas higher energy ions are recorded in a more diffused detector field. The first detector sample was etched for 8 hours. The calibration curve which was taken for this etching time shows that the fusion reaction protons could produce craters of diameters in the range  $4.4-4.8~\mu m$ . In Fig. 2 there are presented two–dimensional track density distributions determined for this sample. The tracks are dispersed in more diffused areas – like triton tracks on the previous detector, and (what is symptomatic) the fusion reaction protons were registered in an annulus area. A similar annulus, like a "picture" of protons source, was obtained in our previous TEXTOR experiment [4, 5].

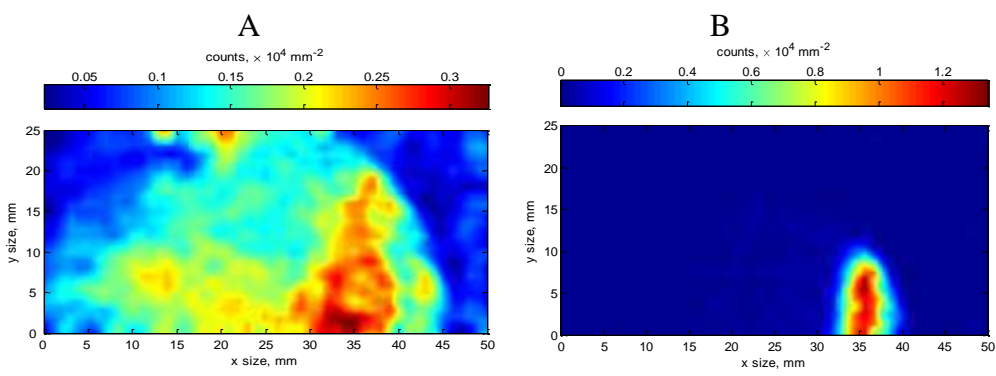


**Figure 1.** Track density distributions upon the second detector sample which was etched only for 2 hours; A – distribution of the craters in the range 1.25 – 1.75 μm, that is those induced probably by fusion reaction tritons, B – distribution of the craters in the range 2.75 – 3.25 μm produced probably by fast primary ions.

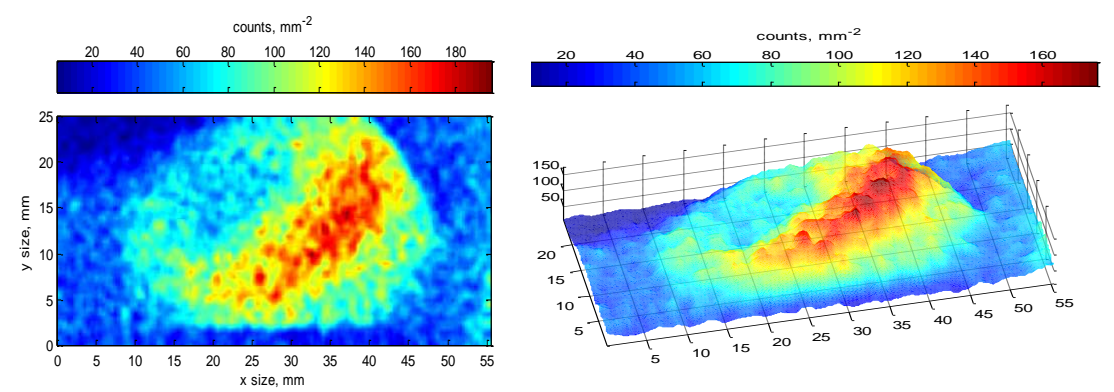


**Figure 2.** Two– and three– dimensional distributions of craters in the range  $4.4 - 4.8 \mu m$ , produced by fusion reaction protons, upon the first detector sample which was etched for 8 hours.

The presented results confirm that the solid-state nuclear track detectors of the PM-355 are useful diagnostic tools for Tokamak experiments, not only for studies of 3-MeV fusion reaction protons but also for measurements of lowest energy ions. The results of the performed calculations have shown that the detection efficiency  $\epsilon_{eff}$  varies in the same way for protons and deuterons of different energies, when it is expressed as a function of the pinhole camera orientation  $\gamma$ . However, the experimental data reveal that the craters induced by lower energy ions are concentrated in a narrower area, whereas higher energy ions are recorded in a more diffused detector field.

#### Conclusions

The results of the described studies can be summarized as follows:

- 1. The PM-355 detector proved to be a quite useful diagnostic tool for tokamak experiments to measure electrically charged particles, both fusion reaction products as well primary ions.
- 2. Track density distributions and track diameter histograms were determined with a good accuracy.
- 3. On the basis of the calibration curves it was possible to distinguish craters produced by protons from other ones, and to convert the obtained histogram into the ion energy spectra.
- 4. The experimental data reveal that the craters induced by lower energy ions are concentrated on the detector surface in a narrower area, whereas higher energy ions are registered in a more diffused detector field.
- 5. It was shown once again that the fusion reaction protons are emitted in an annulus like region.

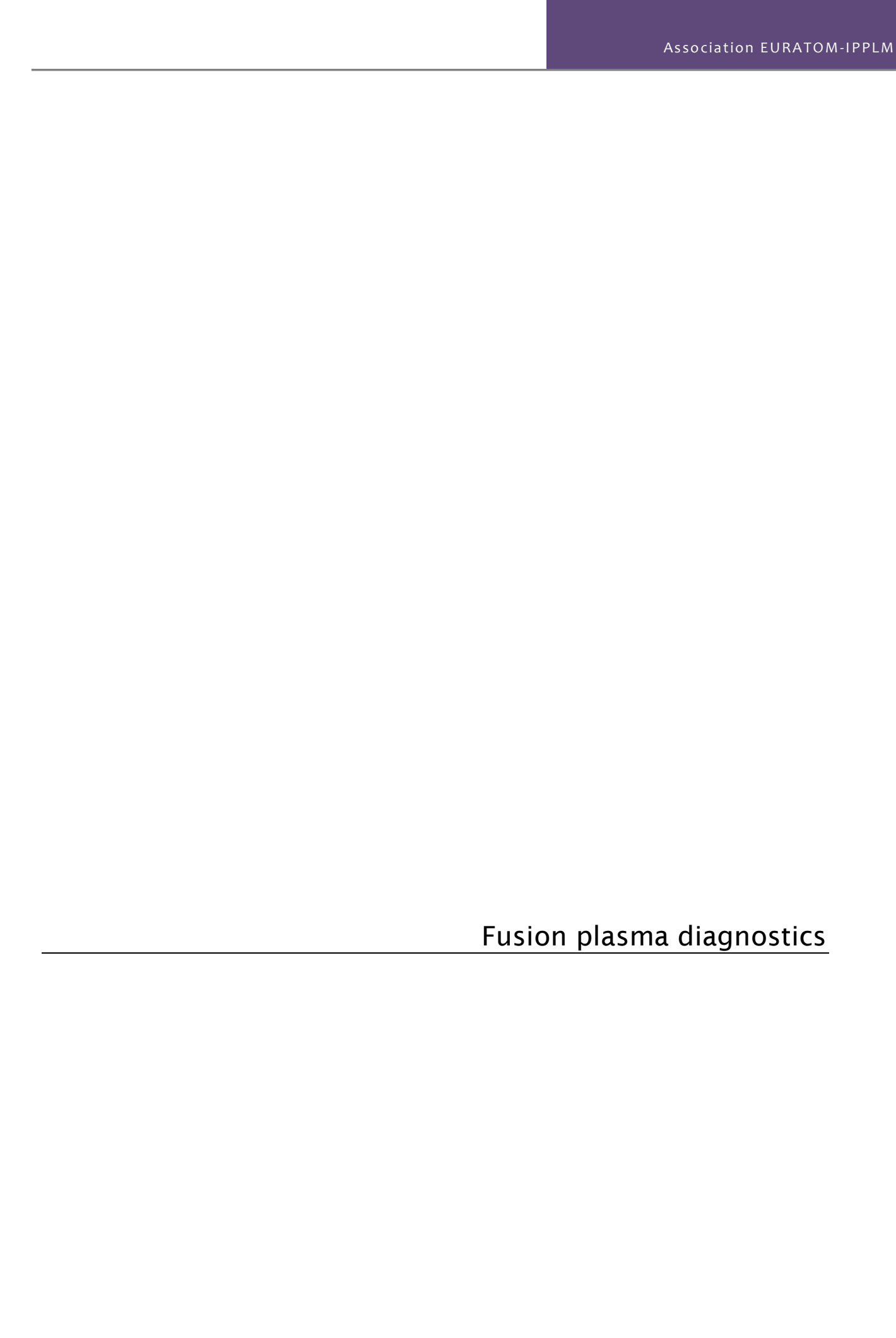
#### Collaboration

<sup>1</sup>Institute of Plasma Physics and Laser Microfusion, Warsaw, Poland Association EURATOM–Belgian State, LPP, ERM/KMS, Trilateral Euregional Cluster, B-1000 Brussels, Belgium Association EURATOM – FZJ, Juelich, Germany

#### References

[1] M. J. Sadowski, et al., Radiat. Meas., Vol.25, Nos 1-4, 175-176 (1995).

- [2] A. Szydłowski, et al., Nucl. Instr. Methods B 171, 379-386 (2000).
- [3] A. Szydłowski, et al., Nucl. Instr. Methods B 149, 113-118 (1999).
- [4] A. Szydłowski, et al., Czech. J. Phys 56, B156-B161 (2006).
- [5] A. Szydłowski, et al., Radiat. Meas. 43, S290-S294 (2008).
- [6] G. Bonheure, et al., Czech. J. Phys 56, B61-B66 (2006).



## 2.6 Spectrometry of soft X-ray emission from W7-X stellarator by the use of fast counting semiconductor detectors

Monika Kubkowska
Institute of Plasma Physics and Laser Microfusion (IPPLM)
mkubkowska@ifpilm.waw.pl

Agata Czarnecka, Sławomir Jabłoński, Jacek Kaczmarczyk, Leszek Ryć, and Jerzy Wołowski

#### **Abstract**

Two spectroscopic systems, the pulse height analysis (PHA) and the multi-foil spectroscopy (MFS), will be applied for measurement of soft X-ray emission from W7-X stellarator built in Greifswald, Germany. The necessary equipment for assembling the experimental PHA system has already been purchased. The first X-ray spectra from the PHA experimental spectrometry system were obtained using the Silicon Drift Detector with a beryllium filter 12.7  $\mu$ m thick. Simulations of X-ray spectra using modified RayX code were made and they contain the contribution of free-free, free-bound and bound-bound transitions. The concept of two spectrometry systems was developed. The diagnostic ports on W7-X for both methods were established.

#### Summary

The subject of the project is to develop and apply two spectroscopic systems for measurement of soft X-ray emission from W7-X stellarator, namely the pulse height analysis (PHA) system and the multi-foil analysis system (MFS). Both systems are needed to obtain the shape of the X-ray spectrum from the data recorded with the use of different detectors and then to estimate the electron temperature of the plasma and the content of heavy impurities. In 2008, the agreement on collaboration between IPPLM, Warsaw, and IPP, Greifswald, in the field of spectrometry of soft X-ray emission from the W7-X stellarator was prolonged up to the year 2010.

In 2008, the equipment necessary for assembling the experimental PHA system was purchased. It was an X-ray spectrometer equipped with a Silicon Drift Detector (SDD). Additionally, a mini X-ray lamp and software for X-ray fluorescence analysis were bought. The testing and calibration of the new spectrometer were done. In the calibration, fluorescence spectra of Cu and Ni foils were measured using the mini X-ray tube.

Some modifications of the RayX code [1], which had earlier been developed at IPPLM for evaluation of X-ray emission from W7-X, were made. The possibility of doing calculations for the specific W7-X plasma geometry and plasma properties was introduced. As the input data for the code, the following parameters are put in: pinhole/sensor position, pinhole sizes, detector types (back illuminated or front illuminated CDD). There is also a possibility to conduct the analysis of the influence of various types of filters on the intensity of the radiation coming to a sensor. As an output, the code generates a set of data for currents and charges for each pixel of the detector in the case of the MFS system and X-ray spectra in the case of the PHA system.

Some simulations of operation of PHA and MFS diagnostics needed at designing these measurement systems were done with the use of the modified RayX code [2]. At the simulations, the geometry of the W7-X, plasma parameters (the distribution of electron temperature and electron density provided by IPP Greifswald), the dimensions of the port used, plasma-pinhole distance, pinhole-detector distance, etc., as well as, the effect of using different filters were taken into account. The simulations were done for the following Be filters: 3, 7, 12.7 and 112.7  $\mu$ m. The simulations gave the possibility to evaluate the influence of main impurities: C, O and Fe, (assumed to be present in W7X plasma) on X-ray emission. The overall concepts of the measuring systems were established [3].

The MFS system will consist of 10 semiconductor detector arrays covered by different filter foils, which will be used for rough reconstruction of X-ray energy spectrum. 10 radial channels will cover a desirable region of central plasma, which takes up about 50 % of the whole plasma radius. This diagnostic will be

realized on the port AEN20 of W7-X. Using the simulation ability of the RayX code, it was possible to consider the behavior of the MFS spectrometer when installed at the W7X. To obtain measurable currents we assumed the distance of the pinhole from plasma to be 2 m and from pinhole to detector 10 cm. The pinhole size was assumed to be 1 mm.

In the case of the X-ray PHA system, it was established that three commercial SDD detectors would be used, each one for different spectral range. We also consider a possibility of the future use of other semiconductors detectors (CdTe, GaAs, InP and diamond), which would be useful for harder energy range and resistant to interfering radiation (neutrons, etc.) [4,5]. For the PHA system, the most important issue is the evaluation of the number of photons which can reach the detector. In preliminary evaluations with the use of the code RayX, a 3-meter distance between plasma and pinhole and 1-meter distance between pinhole and detector were chosen. It was agreed with the IPP side that the PHA system would be mounted on the horizontal port AEK50 of W7-X.

#### Conclusions

In 2008, the agreement on cooperation between IPPLM Warsaw and IPP Greifswald in the field of spectrometry of soft X-ray emission from the W7-X stellarator was prolonged to 2010. Both of the developed spectroscopy methods – MFS and PHA, are complementary. They are useful to obtain the shape of the X-ray spectrum and to estimate space profiles of the electron temperature and density of plasma. The results obtained with the use of simulation RayX code delivered needed information to develop the concept of MFS and PHA spectrometry systems for W7-X. The diagnostic ports on W7-X were chosen. The first X-ray spectra from the experimental spectrometry system developed at IPPLM were obtained.

#### Collaboration

Association EURATOM - IPP, Greifswald, Germany

- [1] S. Jabłoński, A. Czarnecka, J. Kaczmarczyk, L. Ryć, J. Rzadkiewicz, *Assessment of a 1-D, Multi-colour X-ray Imaging System for the MAST ST*, Proceedings of the International Conf. on Research and Appl. of Plasmas "Plasma 2007", Greifswald, Germany 16-19 October 2007, p. 171
- [2] M. Kubkowska, *Results of simulations for MFS and PHA methods using RayX code*, The meeting on X-ray diagnostics for W7-X, 23-24 Sep. 2008, Institute of Plasma Physics and Laser Microfusion, Warsaw. http://www.ipp.mpg.de/eng/for/intern/w7is/proj\_w7xdiag/QX-softX
  - em/QXP\_XPHA/QXP0\_Organization/QXP06\_Meetings\_Protocolls/sep2008/Kubkowska\_Simulations.ppt
- [3] J. Kaczmarczyk, *MFS and PHA diagnostic geometry*, The meeting on X-ray diagnostics for W7-X, 23-24 Sep. 2008, Institute of Plasma Physics and Laser Microfusion, Warsaw. http://www.ipp.mpg.de/eng/for/intern/w7is/proj\_w7xdiag/QX-softX-em/QXP\_XPHA/QXP0\_Organization/QXP06\_Meetings\_Protocolls/sep2008/Kaczmarczyk\_Geometry.pdf
- [4] L. Ryć, L. Dobrzański, F. Dubecky, J. Kaczmarczyk, M. Pfeifer, F. Riesz, W. Słysz, B. Surma, *Application of MSM InP detectors to the measurements of pulsed X-ray radiation*, Radiation Effects and Defects in Solids, vol. 163, Nos. 4-6. April-June 2008, 559-567
- [5] L. Torrisi, D. Margarone, L. Laska, M. Morinelli, E. Milani, G. Verona-Rinati, S. Cavallaro, L. Ryć, J. Krasa, K. Rohlena, J. Ullschmied, *Monocrystalline diamond detector for ionizing radiation emitted by high temperature laser-generated plasma*, Journal of Applied Phys. 103, 083106, 2008.

### 2.7 C-O- monitor for Wendelstein 7-X

Ireneusz Książek
Institute of Physics, Opole University
iksiaz@uni.opole.pl

Adam Bacławski, Tadeusz Kulig, and Józef Musielok

#### **Abstract**

Because of the special properties of soft X-rays (particularly their strong absorpion) the radiation detector is probably the most crucial construction element of the spectrometer working in this spectral range. Because the spectrometer has to demonstrate high temporal resolution, two kind of detectors have been considered for this purpose: a proportional counter and a semiconductor detector. Preliminary tests show that the proportional counter reveals significantly better signal to noise ratio. Moreover, the semiconductor detector turned out to be remarkably sensitive to the scattered light from the infrared spectral range.

#### Summary

For the present study the soft X- ray monochromator "C-O- Monitor for W7-AS", combined with a low voltage X-ray tube, equipped with exchangeable anodes (Al, Cu, and Fe) has been applied. The construction of the monochromator allows to put simultaneously two different detectors in the light path reflected from the dispersive element. The measuring system is equipped with a set of filters and slits mounted in three planes in a common chamber. By turning the adjusting switch, one of the seven different filters can be put into the light beam originating from the X-ray tube.

Preliminary measurements performed by applying the OSI OPTOELECTRONIX XUV-100 diode show that the photocurrent generated in the diode is of the order of picoamperes. Despite of using a high quality electrometer and applying well screened connections, the obtained signal to noise ratio was strongly unsatisfactory.

In order to reduce the influence of outside interference we have decided to apply a preamplifier placed very close to the detector. For this purpose we purchased a measuring setup IRD consisting of the AXUV-100 diode and the preamlifier AXUV-100 HYB1, dedicated to amplify the signal from AXUV-100 photodiode. The construction of this set allows placing the whole set into the vacuum chamber. In this way effective and efficient conversion of low current signals from the diode to voltage signals was feasible.

In spite of these ventures, the measurements show that the signal to noise ratio in the case of applying the diode is still worse compared to the respective ratio obtained with the proportional counter. Moreover, the signal measured from the diode possesses also a strong constant component. Detailed studies show that the high sensitivity of the diode to infrared radiation (scattered radiation in the chamber) is responsible for this constant component. Even the radiation emitted from the "thermovac" instrument (placed above the dispersive element), applied for vacuum control in the chamber, influences the signal detected with the diode significantly.

In order to eliminate the influence of this kind of radiation, usually thin foils (not transparent to long wavelength radiation) are applied. Transmission coefficients determined for different foils applying both measuring systems (semiconductor photodetector, proportional counter) differ considerably. Similar results have been obtained only in the case of very thin Cu and Ni foils. This agreement however, has to be regarded as being accidental. Probably these thin foils are also transparent to long wavelegth (visible) radiation. Applying the thin Be foil in the light path, the intensity measured with the photodiode drops to zero, while the signal measured with the proportional counter decreases only by about 14%. This experiment clearly indicates that the sensitivity of the diode in the soft X- ray range is unsatisfactory. This fact and the relative high sensitivity of the diode for long wavelength radiation leads to the conclusion that this kind of detectors can not be applied for the purpose of monitoring the plasma

radiation of W7-X in the wavelength range where hydrogenlike resonant lines of carbon and oxygen appear.

Table 1. Transmission coefficients determined for K<sub>α</sub>Al (1.49 keV,8.34Å) dla różnych filtrów

Filter set and filter	Filter	Thickness	Trans	mission
number	riner	(µm)	counter	photodiode
1–1	Fe	3	0%	0%
1–2	Hostafan+Al.	6.1	42%	0%
1–3	Be	3	88%	0%
1–4	Al	10	25%	1%
1–5	Al	40	7%	1%
1–6	Cu	0.1	56%	60%
1–7	Ni	0.1	61%	66%
3–1	Hostafan	4	54%	92%
3–2	Al	10	27%	1%
3–3			100%	100%
3–4	Fe	3000	0%	0%
3–5	Cu	3	0%	0%
3–6	Fe	1	4%	0%
3–7	Be	2	86%	0%

#### Conclusions

The application of a proportional counter for monitoring the plasma radiation of W7-X, results in the risk that in case of possible cracks in the entrance window, the counter gas may contaminate the measuring setup. Moreover, the necessity of using very thin foils in front of the counter is connected with small, but noticeable penetration of the counter gas into the plasma. However, undoubtedly the main advantage of proportional counters are their very small level of noises. The high sensitivity in the long wavelength range and the unsatisfactory signal to noise ratio, found for the semiconductor detector, determined our final decision – the proportional counter will be applied for soft X- ray detection in the construction of the C-O- Monitor for W7X.

#### Collaboration

Association EURATOM – IPP, Greifswald, Germany

### 2.8 Microwave diagnostic development

Yury A. Kravtsov

Maritime University of Szczecin, Poland
kravtsov@am.szczecin.pl

Bohdan Bieg, Paweł Berczyński<sup>1</sup>, and Janusz Chrzanowski

#### **Abstract**

Two basic theoretical methods in microwave plasma polarimetry are presented: quasi-isotropic approximation (QIA) and Stokes vector formalism (SWF). Both methods describe polarization of electromagnetic waves in weakly anisotropic plasma.

QIA stems directly from the Maxwell equations under assumption of weak anisotropy and deals with coupled differential equations for the transverse components of the electromagnetic wave field. Being applied to high frequency (microwave or IR) electromagnetic waves in magnetized plasma, QIA describes combined action of Faraday and Cotton-Mouton phenomena. QIA takes into account curvature and torsion of the ray, describes normal modes conversion in the inhomogeneous plasma and allows specifying area of applicability of the method.

In distinction to QIA, Stokes vector formalism (SVF), developed by Segre on the basis of Azzam approach, deals with quantities quadratic in a wave field. It is shown that Segre-Azzam equation for Stokes vector evolution, which actually corresponds to weakly anisotropic plasma, can be derived directly from QIA. This evidences deep unity of two seemingly different approaches to plasma polarimetyry. In fact QIA suggests somewhat more information than SVF; in particular, it describes the phases of both transverse components of the electromagnetic field, whereas SVF operates only with the phase differences.

Besides, researches were continued on microwave diffraction processes in the inhomogeneous plasma and new studies were undertaken, concerning plasma tomography of higher resolution.

#### Summary

Coupled wave equations for the components of the electromagnetic wave field in the weakly anisotropic media were suggested in [1] in the form of quasi-isotropic approximation (QIA) of the geometrical optics method. QIA was developed in depth in subsequent publications [2,3] and briefly outlined in the books [4,5]. Exemplary applications of QIA are presented in [6-10]. An alternative approach – "Stokes vector formalism" (SVF) – initiated in the papers [11,12], was applied for analysis of electromagnetic waves polarization in the inhomogeneous plasma [13]. Comparative analysis of two approaches mentioned have been performed by Serge [14], who has analyzed advantages and shortcomings of each technique, omitting yet their deep unity. Our research proved that equations for evolution of the four-component Stokes vector in weakly anisotropic and smoothly inhomogeneous media can be obtained on the basis of quasi-isotropic approximation of the geometrical optics method [9,10,15,16]. In the report we present:

- brief outline of QIA approach,
- derivation of the equations for Stokes vector evolution  $\dot{\mathbf{s}} = \Omega \times \mathbf{s}$  from the equations of Quasi-Isotropic Approximation of geometrical optics method

$$\begin{cases} \dot{\Gamma}_{1} = \frac{1}{2}ik_{0}\varepsilon_{0}^{-1/2}(\nu_{11}\Gamma_{1} + \nu_{12}\Gamma_{2}) \\ \dot{\Gamma}_{2} = \frac{1}{2}ik_{0}\varepsilon_{0}^{-1/2}(\nu_{21}\Gamma_{1} + \nu_{22}\Gamma_{2}) \end{cases}$$

- distinctions between these two approaches and simultaneously their practical equivalence in conditions, when the total phase of the wave field is not significant,
- an example of numerical calculations the polarization changes in the case of normal mode conversion in the tokamak plasma

Studies of microwave diffraction in the inhomogeneous plasma were continued, started in 2006 and 2007. In particular, the solutions for eigen waves in inhomogeneous planar plasma waveguide with

parabolic profile of electric permittivity was obtained, using the complex geometrical optics method (CGO), which deals with the ordinary differential equations [17].

In 2008 studies of plasma tomography of higher resolution were started in collaboration with the Irkutsk State University, Russia [18-20]. Double weighted Fourier transform (DWFT) method is suggested to extract the line-integral of the electron density in the turbulent plasma from microwave data.

#### Collaboration

<sup>1</sup>West Pomerania University of Technology, Szczecin, Poland Association EURATOM – IPP, Greifswald, Germany Association EURATOM – UKAEA Culham Science Center, Abingdon, UK Irkutsk State University, Russia.

- [1] Yu.A. Kravtsov, Sov. Phys. Doklady, 13(11), 1125-1127 (1969).
- [2] Yu.A. Kravtsov, O.N. Naida and A.A. Fuki, Physics-Uspekhi, 39(2), 129-134 (1996).
- [3] A.A. Fuki, Yu.A. Kravtsov and O.N. Naida, *Geometrical Optics of Weakly Anisotropic Media*, Lond., N.Y., Gordon & Breach, 1997.
- [4] Yu.A. Kravtsov and Yu.I. Orlov, *Geometrical optics of inhomogeneous media*, Berlin, Heidelberg, Springer Verlag, 1990.
- [5] Yu.A. Kravtsov, Geometrical Optics in Engineering Physics, London, Alpha Science, 2005.
- [6] Yu.A. Kravtsov, B. Bieg, 16th Polish-Slovak-Czech Optical Conference on Wave and Quantum Aspects of Contemporary Optics, edited by A. Popiolek-Masajada, E. Jankowska, W. Urbanczyk Proc. of SPIE Vol. 7141, 71410K-1/8 (2008).
- [7] Yu.A. Kravtsov, B. Bieg, Z. H. Czyz, *Proceedings of the International Radar Symposium IRS-2008*, 21-23 May 2008, Wroclaw, Poland, Ed.A. Kawalec and P. Kaniewski, pp.37-40 (2008).
- [8] Yu.A. Kravtsov, B. Bieg, *Progress in the theory of microwave plasma polarimetry*. Seventh Kudowa Summer School "Towards Fusion Energy: Plasma Physics, Diagnostics, and Technology". Kudowa Zdroj, Poland, June 20-24, 2008.
- [9] K.Yu. Bliokh, D.Yu. Frolov and Yu.A. Kravtsov, Phys. Rev. A, 75, 053821 (2007).
- [10] Yu. A. Kravtsov, B. Bieg and K. Yu. Bliokh, J. Opt. Soc. Am. A, 24, 3388 (2007).
- [11] G.N. Ramachandran and S. Ramaseshan, Crystal Optics. Encyclopedia of Physics 25/1, Berlin, Springer, 1961.
- [12] R.M.A. Azzam, J. Opt. Soc. Am. 68, 1756-1767 (1978).
- [13] S.E. Segre, Plasma Phys. Control. Fusion 41, R57–R100 (1999).
- [14] S.E. Segre, Preprint RT/ERG/FUS/2001/13, 2001, ENEA, Frascati, Italy (2001).
- [15] Yu.A. Kravtsov, B. Bieg, Cent. Eur. J. Phys. 6(3), 563-568 (2008).
- [16] Yu.A. Kravtsov, B. Bieg, K. Yu. Bliokh, and M. Hirsch, *Proceedings of the International Conference on Research and Applications of Plasmas*, Greifswald, Germany, 16-10 Oct 2007, ed. by H-J Hartfuss, M. Dudeck, J. Musielok, M. J. Sadowski. AIP Conference Proceedings, 993, 134 (2008).
- [17] P. Berczyński, Yu.A. Kravtsov, G. Żegliński, Cent. Eur. J. Phys. 6(3), 603-611 (2008).
- [18] M.V. Tinin, Yu.A. Kravtsov, Plasma Phys. Control. Fusion, 50, 035010 (2008).
- [19] Yu.A. Kravtsov, M.V. Tinin, A.V. Kulizhsky, Fusion Engineering and Design, 2008, DOI: 10.1016/j.fusengdes.2008.11.033
- [20] Yu.A. Kravtsov, M.V. Tinin, K. Makles, 16th Polish-Slovak-Czech Optical Conference on Wave and Quantum Aspects of Contemporary Optics, edited by A. Popiołek-Masajada, E. Jankowska, W. Urbańczyk, Proc. of SPIE Vol. 7141, 714120-1/6 (2008).

### 2.9 Detection of the delayed neutrons from activation of fissionable materials in the neutron field at fusion-plasma devices

Krzysztof Drozdowicz The Henryk Niewodniczanski Institute of Nuclear Physics Polish Academy of Sciences krzysztof.drozdowicz@ifj.edu.pl

Andrzej Drabina, Barbara Gabańska, Andrzej Igielski, Władysław Janik, Arkadiusz Kurowski, Urszula Wiącek, Urszula Woźnicka, and Jan Dankowski

#### **Abstract**

Measurement of the delayed neutrons, which are emitted from tablets of fissionable materials irradiated in a field of neutrons originated in thermonuclear plasma, is supplementary to the known neutron activation method for fusion plasma diagnostics. A basic design of the device for detection of the delayed neutrons has been optimized in respect of positions of the neutron detectors in a moderator (polyethylene) layer and of the width of this layer. A technical project of the device has been completed, a system of neutron detectors and electronic and data collection systems have been designed.

#### Summary

One of principal methods for neutron-based techniques for *fusion plasma diagnostics* is the neutron activation technique based on the gamma spectrometry of the activated samples. Data from a measurement of delayed neutrons from fissionable isotopes irradiated in a field of neutrons originated in thermonuclear plasma supplements the neutron activation method. We designed a device for measuring the delayed neutrons, thought to be used in a plasma diagnostic systems at the new-generation stellarator, Wendelstein 7-X (under construction in the Max-Planck-Institute for Plasma Physics, Greifswald Branch). A physical base of the method for generation and measurement of delayed neutrons was presented in [1]. Such isotopes as <sup>235</sup>U, <sup>238</sup>U or <sup>232</sup>Th, irradiated with neutrons, emit prompt neutrons at the fission act (~99 %) and later the delayed neutrons (~1%) from the fission products which decay with the beta-emission. Total efficiency of a final detection of the delayed neutrons depends not only on the number and efficiency of particular neutron detectors but also on positioning of the detectors

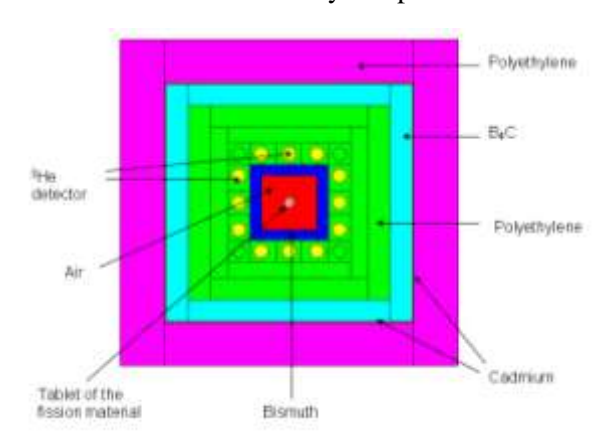


**Figure 1** Schematic horizontal cross section of the setup for the delayed neutron detection.

in a principal moderator layer and on the width of this layer. The layer which is too thin does not deliver a sufficient number of thermal neutrons. On the other hand, if neutron travel paths in a thick layer before hitting the detector are too long then a probability of absorption and unprofitable scatterings increases. These problems have been considered and numerous Monte Carlo computer simulations have been performed using the MCNP code.

A conceptual scheme of the delayed neutron measuring device is reminded in Fig 1. Purposes for the use of layers of particular materials were given in [1]. The 3He neutron detectors were assumed for the delayed neutron detection.

A Monte Carlo simulation of the entire process – irradiation, fission, emission of delayed neutrons and then their slowing down, diffusion and detection – is strongly time consuming because of the small contribution of the delayed neutrons. This full modelling is unacceptable when a big number of simulations is to be done for optimization of the measuring arrangement. Therefore, the modelling is divided in two phases: i) generation of delayed neutrons by irradiation of the fissionable material sample, and ii) treating the sample as a primary source with well-defined energy and time distributions of neutrons. The time distributions (a decay in time) of delayed

neutrons escaping the irradiated fissionable material samples have been obtained as well as the energy distributions of these neutrons for 232Th, 235U, and 238U. Apart of differences of the intensities and positions of individual maxima one can observe that in all cases most delayed neutrons escaping the tablets have energies below 0.5 MeV.

A placement of the 3He detectors within the neutron moderating polyethylene layer has been optimized. The delayed fast neutrons has to be slowed down to thermal energies to be detected in the 3He detectors. Maximum of the space distribution of thermal neutrons in the moderating layer should arrive at the detectors. The thicker is the moderator layer the higher is efficiency of moderating neutrons. But the

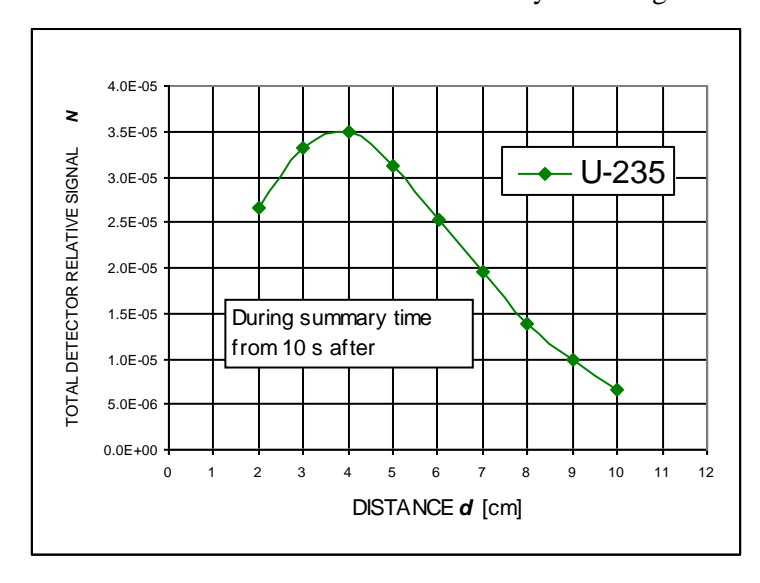


**Figure 2** Total detector signal as a function of the position *d* of the detectors (integrated over the time from 10 s after irradiation of the U-235 sample).

isotope used. An example for 235U is shown in Fig. 2.

An optimum thickness of the polyethylene moderator layer should also be defined. The amount of polyethylene behind the detectors (while looking from the centre) must not be too small if it has to take a significant participation in moderating and reflecting neutrons. On the other hand, some parts of the layer too distant are useless as they do not gain the thermal neutron flux at the detectors and enlarge unnecessary amount of the material, which enlarges a total mass of the device and gives no profit. Monte Carlo simulations of the detector answer have been performed varying the width of the polyethylene layer w from 6 to 13.5 cm. The total size of the inner polyethylene part of device changes then the

longer is neutron path in the moderator the stronger is absorption and higher is number of unprofitable scatterings (escape of neutrons outside the layer or a longer travel path). A width of the layer behind the detector also influences the detection acting still as the moderator and also as the reflector of neutrons.

The boundary between the bismuth and polyethylene layers has been taken as a reference point for definition of a depth of the detector position, d, inside the layer. Series of simulations of the neutron transport have been made. Typical 3He detectors have been considered: a 1 inch diameter, a 25 cm active length and a 5 atm. pressure. The distance d of the detector axis from this inner boundary surface has been varied from 2 to 10 cm. The optimum has been found at d = 3÷4 cm, depending on the

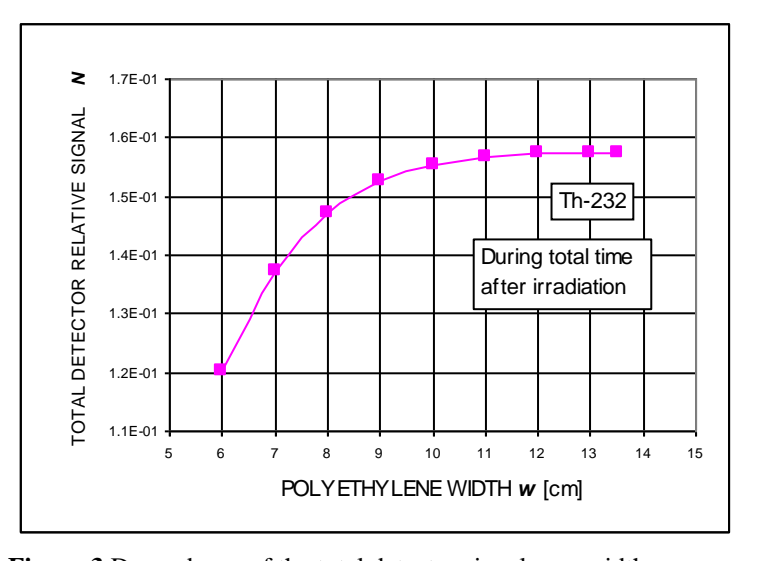


**Figure 3** Dependence of the total detector signal on a width w of the moderator layer (integrated over the total time after irradiation of the Th-232 sample).

21x21x33 cm3 up to 36x36x48 cm3. An example result of the simulations is presented in Fig. 3. An enlargement of the moderator layer width over 12 cm does not increase the detector signal.

A technical design of the measuring chamber has been performed according to results of former and of the presented optimizations. Some minor changes have been made because of properties of available materials. The specification is following.

- → General external dimensions of the device are: square horizontal size 58x58 cm², height 74 cm.
- $\rightarrow$  Hole for the pneumatic transport: 6x6 cm<sup>2</sup>.
- → Consecutive layers from the hole towards outside:
- → Bismuth: 2 cm; Polyethylene (moderator): 12 cm; B<sub>4</sub>C (absorber): 3.8 cm;
- → Cadmium (absorber): 0.2 cm; Polyethylene (external protection): 8 cm.
- → <sup>3</sup>He neutron detectors: 12 pcs., 1" diameter, 30 cm length (25 cm active), 5 atm. pressure.

An electronic system for the neutron detection and data collection has been designed. As mentioned, the delayed neutrons contribute in only ~1% of the secondary emission from the irradiated tablets. Thus, the expected intensity of counts in the 3He detectors will be rather low. Therefore, we have decided to use a system in which three 3He detectors are coupled to one preamplifier. Then the preamplifiers in a usual way are connected to amplifiers and they to a digitizer card in a PC.

#### Conclusions

Sizes of important parts of the measuring chamber have been optimized to achieve the delayed neutron detection as efficient as possible. The delayed neutron transport from irradiated tables of fissionable materials has been modeled with the Monte Carlo method. A signal of detectors has been found as a function of their position in the neutron moderating layer of polyethylene and as a function of this layer width. The three potential materials (235U, 238U, 232Th) have been considered. A sufficient width of the moderator layer has been estimated to 12 cm. The optimum distance of detectors from the inner boundary of the moderator is 3÷4 cm.

A technical project of the device is made according to the obtained optimizations.

Full simulations of the neutron transport in the measuring device will be repeated later using dimensions and material parameters of all parts as used in the final construction. For purposes of a future elaboration of a method of interpretation of measurement results a particular attention have to be turned out to a problem of accuracy of nuclear cross sections of acting materials [8].

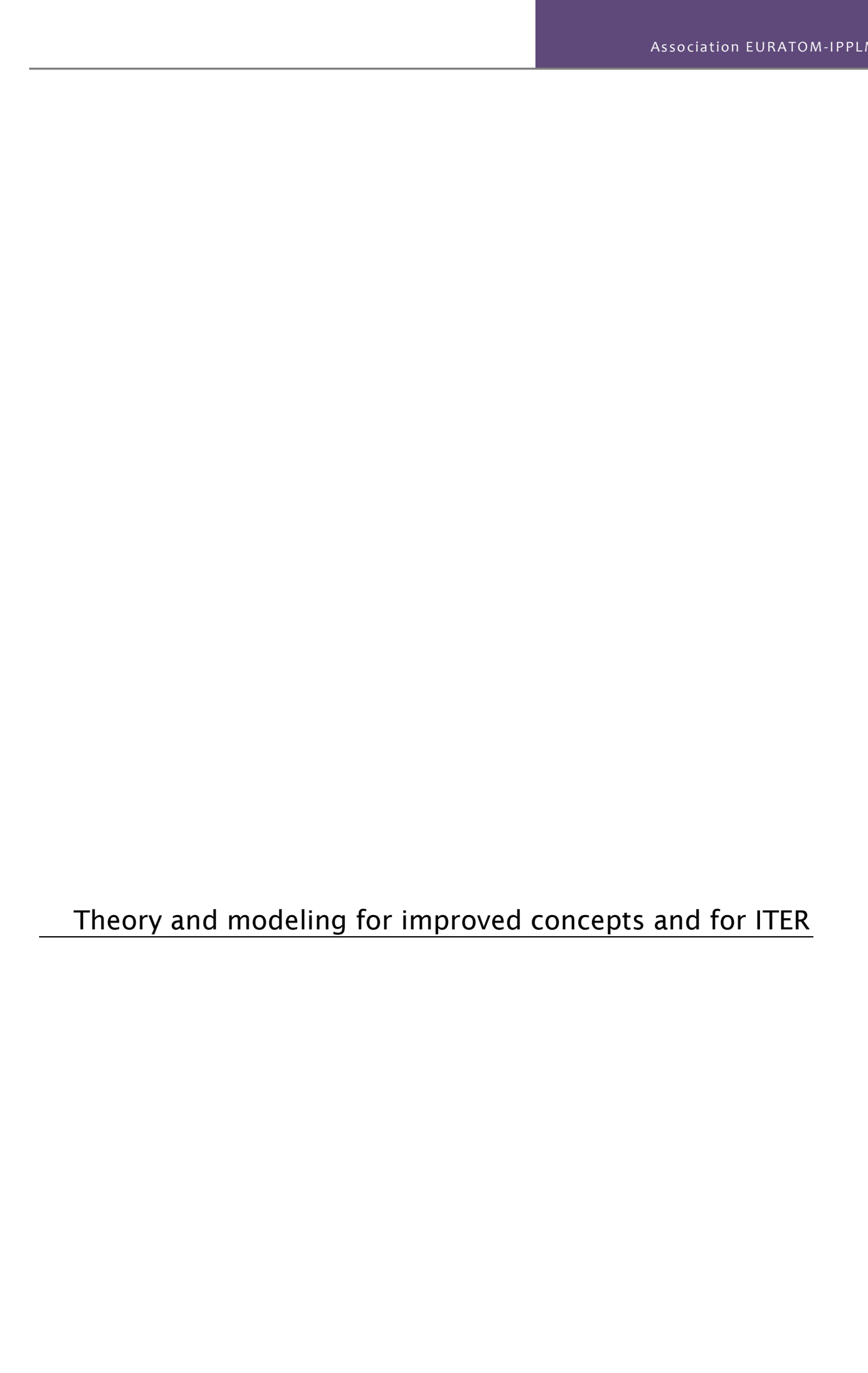
A complete electronic system for the neutron detection and data collection has been designed and its parts have been acquired. The next step will be to test particular elements (in particular, a compliance of detectors in groups of three) and to compose the system.

#### Collaboration

Association EURATOM – IPP, Greifswald, Germany Association EURATOM – UKAEA Culham Science Center, Abingdon, UK

#### Reference

[1] K. Drozdowicz, et al., *Detection of the delayed neutrons from activation of fissionable materials in the neutron field at fusion-plasma devices*, Ann. Rept. 2007 of the Assoc. EURATOM-IPPLM, Warsaw, 2008, 38; and CD-R 2\_11\_Areport\_2007.pdf, 14 pp.



## 2.10 Nonlinear dynamics of fast ion driven plasma modes near instability threshold – theoretical basis for integrated tokamak modelling

Irena Kruk West Pomerania University of Technology Irena.Kruk@ps.pl

Jarosław Zaleśny<sup>1</sup>, Sławomir Marczyński, Paweł Berczyński, and Stefan Berczyński

#### **Abstract**

In 2008, working in collaboration with Prof. M. Lisak and Prof. P. Helander on the P11 project, we made the bases for generalization the existing nonlinear model of fast ion driven plasma modes for multi-mode case. Within this model on example of two interacting modes we observed modes competition and beats. Moreover, we simplified the integro-differential single mode equation to an ordinary differential equation. The universal integro-differential model equation derived by H. Berk and B. Breizman et al. in [1] for studying the nonlinear evolution of unstable modes driven by kinetic wave particle resonances near the instability threshold has been reduced to a differential equation and next after further simplification to a nonlinear oscillator equation. This mechanical analogy properly reproduces most of the essential physics of the system and allows an understanding of the qualitative features of the Berk and Breizman theory. In this simplified model the multi-mode plasma waves can be analyzed by means of analogy with coupled nonlinear mechanical oscillators.

#### Summary

The multi-mode case has been considered in 2008 in the case of (BB) equation [1] on the example of two coupled modes and mode competition effect as well as beats has been observed (Fig. 1).

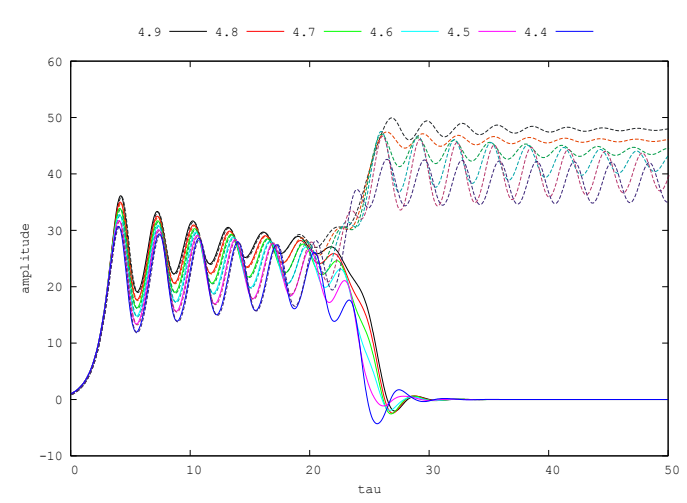


**Figure 1**. The mode competition effect. Initial conditions: A1(0)=1, A2(0)=exp( $i\pi/6$ ), 4.4< $\hat{V}$ <4.

In the case of greater number of modes the multi-mode theory has been based on the differential equation approach. The (BB) single-mode problem can be simplified to solving the ordinary differential equation:

$$\frac{d}{dt} \left\{ \frac{1}{xe^{\nu t}} \frac{d^3}{dt^3} [(\dot{x} - \gamma x)e^{2\nu t}] \right\} = -\gamma_L x^2 e^{\nu t} \tag{1}$$

which after further simplifications can be reduced to the Duffing-Van der Pol nonlinear oscillator of the following form:

$$12.8 \ \nu^3 \ \ddot{x} + \left(\nu^3 (8\nu - 19.1\gamma) - 2.7 \frac{\gamma_L}{\nu} x^2\right) \ \dot{x} - 8\nu^4 \gamma \ x + \gamma_L \ x^3 = 0 \tag{2}$$

The above equation (2) posses main features of (BB) equation [1]. Thus, it contains the essential physics of the (BB) theory. For instance the blow-up behaviour can be observed (Fig. 2).

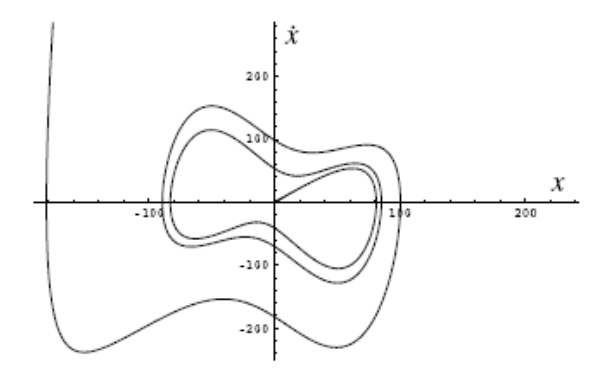


**Figure 2.** The phase portrait of equation (4); blow-up behaviour.

It can be shown that simplified multi-mode model can be considered as the system of coupled nonlinear oscillators of Duffing-Van der Pol type.

The multi-mode case has been considered in 2008 in the case of (BB) equation on the example of two coupled modes. In the case of greater number of modes the theory has been based on the differential equation approach. The further analysis of multi-mode model of fast ion driven plasma waves will be realized in 2009 both on the basis of (BB) type integral equations and simplified ordinary differential equations approach.

#### Conclusion

We worked out the basis for the analysis of the multi-mode case on the simplified differential equations approach. In the approach of (BB) integral equations in multi-mode case we observed mode competition and beats in numerical solutions shown on the example of two waves amplitudes. Our results are going to be published in 2009 in a appropriate journal.

#### Collaboration

<sup>1</sup>Institute of Plasma Physics and Laser Microfusion, Warsaw, Poland Association EURATOM – VR, Chalmers University of Technology, Göteborg, Sweden Association EURATOM – IPP, Greifswald, Germany

#### References

[1] H. L. Berk et al., *Nonlinear Dynamics of a Driven Mode near Marginal Stability*, Phys. Rev. Lett. 8(76)1996, pp 1256-1259.

## 2.11 Stochastic processes and stochastic representations for the kinetic equations of a gas of charged particles

Witold Karwowski
Institute of Physics, Opole University
witoldkarwowski@go2.pl

#### **Abstract**

In this note we illustrate an effective way to construct the transition function from a given Dirichlet form. The construction is valid for the models of hierarchical spaces corresponding to the *p*-adic unite balls.

#### Summary

This material is based on ref. [1] by reversing the reasoning i.e. going from the Dirichlet form to the transition function. Recall that for any prime number p the symbol  $\mathbb{Q}_p$  stands for the field of p-adic numbers.

Define a sequence  $a(M), M \in \mathbb{Z}$  such that  $a(M+1) \leq a(M)$  and  $a(M) \to_{m \to \infty} 0$ . Let  $\alpha$  be a set function on the balls in  $\mathbb{Q}_p$  defined by  $\alpha(K(a,p^M)) = p^M$ , where  $K(a,p^M) = \{x \in \mathbb{Q}_p, \|x-a\|_p \leq p^M\}$ . Then  $\alpha$  extends uniquely to the Haar measure (with respect to p-adic translation) on  $\mathbb{Q}_p$ . When integrating with this measure we write dx. Consider real Hilbert space  $L^2(\mathbb{Q}_p, dx)$  and the form defined by

$$E(\chi_{K(a,p^N)}, \chi_{K(b,p^N)}) = \int_{\mathbb{Q}_p \times \mathbb{Q}_p \setminus d} (\chi_{K(a,p^N)}(x) - \chi_{K(a,p^N)}(y)) (\chi_{K(b,p^N)}(x) - \chi_{K(b,p^N)}(y)) J(dx, dy)$$
(1)

where 
$$||a - b||_p = p^n$$
 and  $n > \max\{M, N\}$  and  $J(K(a, p^M), K(b, p^N)) = \frac{1}{2}p^{N+M-n+1}(a(n-1) - a(n))$ 

E extended by linearity is closable and its closure is a Dirichlet form in  $L^2(\mathbb{Q}_p, dx)$ . Put H for the corresponding s.a. operator.

By direct computations we find

$$E(\chi_{K(a,p^N)}, \chi_{K(a,p^N)}) = p^N a(N)$$
(2)

Suppose the functions  $\chi_{K(a,p^N)}$ ,  $a \in \mathbb{Q}_p$ ,  $N \in \mathbb{Z}$  belong to the domain of H then

$$E(\chi_{K(a,p^M)}, \chi_{K(b,p^N)}) = \int_{\mathbb{O}_n} \chi_{K(a,p^M)}(x) (H\chi_{K(b,p^N)}(x)) dx$$
 (3)

implies

$$H\chi_{K(b,p^M)}(x) = -p^{N-m+1}(a(M+m-1) - a(M+m))$$
 (4)

iff  $\|b-x\|_p=p^{M+m}, m\in\mathbb{N}$  . Moreover (2) implies

$$H\chi_{K(b,p^N)}(x) = p^N a(N) \tag{5}$$

iff  $x \in K(b, p^N)$ . Using (4)and (5) one finds the orthonormal basis  $e_M^k$  of eigenfunctions and  $h_M$  the corresponding eigenvalues for H. Both given explicitly. The transition function is defined as follows. Let  $x \in K(0, p^N)$  then

$$P_{t}(x, K(0, p^{N})) = e^{Ht} \chi_{K(0, p^{N})}(x)$$

$$= \sum_{M=N}^{\infty} \sum_{k=0}^{p-2} (\chi_{K(0, p^{N})}, e_{M}^{k}) e^{-h_{M}t} e_{M}^{k}(x)$$

$$= \sum_{M=N}^{\infty} \frac{p-1}{p} p^{N-M} e^{-h_{M}t} = \frac{p-1}{p} \sum_{i=0}^{\infty} p^{-h_{i+N}t}$$

$$= \frac{p-1}{p} \sum_{i=0}^{\infty} p^{-i} \exp \{-(p-1)^{-1} [pa(N+i) - a(N+i+1)]t\}.$$
(6)

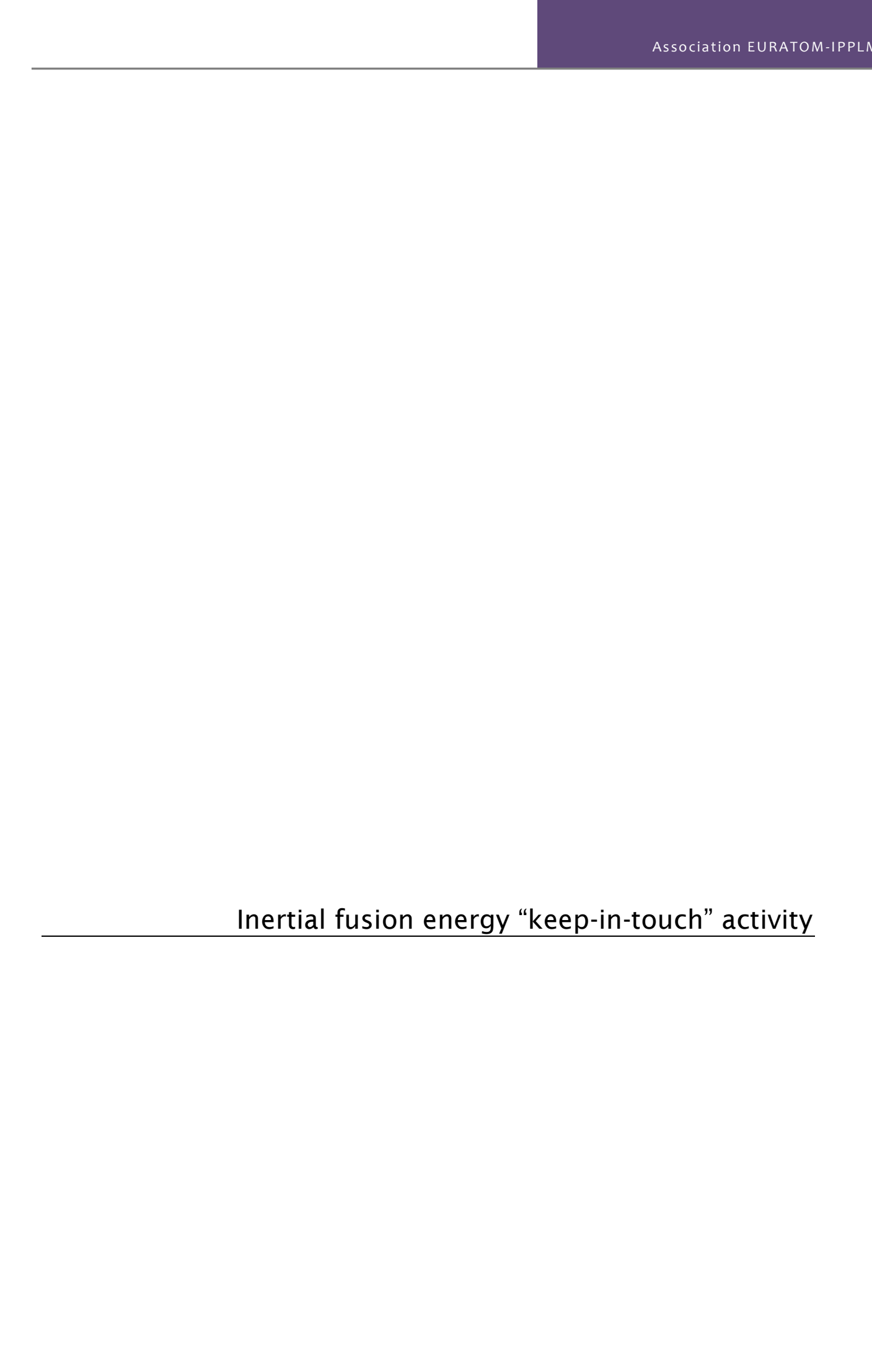
This is formula (3.1) of ref. [1], where it had been obtained by solving the Chapman-Kolmogorov equations. The formula for  $P_t(x, K(0, p^N))$  when  $x \notin K(0, p^N)$  is given by (3.2) of [1] obtained according to (2.35).

#### Collaboration

Association EURATOM – CEA, Marseille, France

#### References

[1] S. Albeverio, W. Karwowski. A random walk on p-adics - the generator and its spectrum. Stochastic Processes and their Applications 53(1994)1-22.



### 2.12 Studies on fast ignition of inertial fusion using laser-driven proton beams

Jan Badziak Institute of Plasma Physics and Laser Microfusion, Warsaw, Poland badziak@ifpilm.waw.pl

J. Wołowski, A. Borrielli <sup>4</sup>, L. Dareshwar <sup>2</sup>, I. B. Foldes <sup>3</sup>, A. Kasperczuk, E. Krousky <sup>1</sup>, L. Laska <sup>1</sup>, K. Masek <sup>1</sup>, A. Mezzasalma <sup>4</sup>, P. Parys, M. Pfeifer <sup>1</sup>, T. Pisarczyk, M. Rosiński <sup>1</sup>, L. Ryć, R. Suchańska, T. Suta <sup>3</sup>, L. Torrisi <sup>4</sup>, J. Ullschmied <sup>1</sup>, and P. Pisarczyk

#### **Abstract**

Acceleration of a thin (10 or 20  $\mu$ m) plastic foil by 120 J, 0.438  $\mu$ m, 0.3 ns laser pulse of intensity up to  $10^{15} \text{W/cm}^2$  has been investigated. It is shown that the introducing a high-Z dopant to the foil causes an increase in the ablating plasma density, velocity and collimation which, in turn, results in a remarkably higher kinetic energy and energy fluence of the flyer foil. The obtained results demonstrate that laser-accelerated macroparticle containing a high-Z dopant can achieve very high velocities necessary for efficient impact fast ignition.

#### Summary

Impact fast ignition of inertial fusion requires that a macroparticle of sufficiently high density and mass is accelerated by laser-induced plasma ablation to velocities above 108 cm/s [1, 2]. The main obstacle in achieving such macroparticle velocities (which has never been attained before) is the Rayleigh-Taylor (RT) instability [3], which prevents the macroparticles from stable acceleration and it can destroy them before colliding with the precompressed DT fuel. One of the possible ways to suppress the RT instability and, as a result, to increase the macroparticle parameters is using laser-induced double plasma ablation (created by the laser light and the X-rays from a high-Z dopant introduced to a low-Z target) [4, 5]. It has been demonstrated recently that a plastic thin foil disc (a macroparticle) doped with a small amount ( $\sim$  3% weight) of high-Z atoms (Br) and irradiated by 0.35- $\mu$ m, 2.5-ns, 10<sup>14</sup> W/cm<sup>2</sup> laser pulse could be accelerated to a record velocity of 6×10<sup>7</sup> cm/s [2], which was remarkably higher than that for an undoped disc. However, it was not confirmed that the densities of the accelerated discs were similar for both cases and, that the kinetic energy of the high-Z doped disc was also higher.

The objective of the studies was to demonstrate that using laser-induced double plasma ablation (created by the laser light and the X-rays from a high-Z dopant introduced to a low-Z target) it is possible to increase significantly the kinetic energy of a macroparticle accelerated by a laser. In the experiments, the high-intensity (1014 – 1015W/cm<sup>2</sup>), high-energy (up to 120 J) sub-ns 3ω beam of the PALS laser[6] interacted with various (with and without high-Z dopant) thin foil targets. The laser-driven foil (the "macroparticle") collided with a massive (Al) target producing crater, the volume of which was a measure of the foil kinetic energy released to the foil. Parameters of the accelerated foil and the ablated plasma were determined using three-frame interferometry [7], ion diagnostics [8], soft and hard X-ray diagnostics [9] as well as the measurements of the crater dimensions. The results of investigations for low-Z foil targets; for undoped (homogenous) and for ones with high-Z dopants, were compared. It was found that the X-ray yield from the foil target with high-Z dopant is a few times higher than that from the undoped target and the ablating plasma flow is faster and more collimated. It results in an increase in kinetic energy of the accelerated foil (the crater volume is up to 80% larger) provided that the foil is sufficiently thick (20 µm). Higher increase in the kinetic energy seems to be possible when using foils with a higher amount of a high-Z dopant and the foil thickness is well matched to the laser beam parameters.

#### Conclusions

It has been found that the ablating plasma flow from the high-Z doped foil target moves faster and more collimated and the plasma has a higher density than in the case of undoped target. It results in higher kinetic energy and/or density of the flyer foil at the late phase of acceleration (at the moment of the foil-massive target collision) in case the foil is sufficiently thick. The observed increase in the flyer foil performance is likely caused by additional plasma ablation created deep in the foil by X-ray radiation, which is measured to be significantly more intense in the case of high-Z doped target. Even larger increase seems to be possible with this method when using foils with a higher amount of a high-Z dopant and the foil thickness is well matched to the laser beam parameters. The obtained results demonstrate that laser-accelerated macroparticle containing a high-Z dopant can achieve very high velocities necessary for efficient impact fast ignition.

#### Collaborations

<sup>1</sup>PALS Research Center, AS CR, Prague, Czech Republic

<sup>2</sup> Bhabha Atomic Research Centre, Mumbai, India

<sup>4</sup> University of Messina, Faculty of Physics, Messina, Italy.

- [1] M. Murakami and H. Nagatomo, 2005 Nucl. Inst. and Meth. Phys. Res. A 544 67-75
- [2] M. Murakami, H. Nagatomo, H. Azechi, F. Ogando, M. Perlado and S. Eliezer, 2006 Nucl. Fusion 46 99-103
- [3] A. Atzeni and J. Meyer-ter-Vehn, 2004 Physics of Inertial Fusion, Clarendon Press, Oxford
- [4] S. Fujioka, A. Sunahara, K. Nishihara, N. Ohnishi, T. Johzaki, H. Shiraga, K. Shigemori, M. Nakai, T. Ikegawa, M. Murakami, K. Nagai, T. Norimatsu, H. Azechi and T. Yamanaka, 2004 Phys. Rev. Lett. 92 195001
- [5] H. Azechi, H. Shiraga, M. Nakai, K. Shigemori, S. Fujioka, T. Sakaiya, Y. Tamar, K. Ohtan, M. Murakam, A. Sunahara, H. Nagatomo, K. Nishihara, N. Miyanaga and Y. Izawa, 2004 Plasma Phys. Control. Fusion 46 B245-B254
- [6] K. Jungwirth, A. Cejnarova, L. Juha, B. Kralikova, J. Krasa, E. Krousky, P. Krupickova, L. Laska, K. Masek, T. Mocek, M. Pfeifer, A. Präg, O. Renner, K. Rohlena, B. Rus, J. Skala, P. Straka and J. Ullschmied, 2001 Phys. Plasmas 8, 2495-2501
- [7] A. Kasperczuk and T. Pisarczyk, 2001 Opt. Appl. 31 571
- [8] J. Wołowski, J. Badziak, F.B. Boody, H. Hora, V. Hnatowicz, K. Jungwirth, J. Krása, L. Láska, P. Parys, V. Perina, M. Pfeifer, K. Rohlena, L. Ryć, J. Ullschmied and E. Woryna, 2002 Plasma Phys. Control Fusion 44 1277
- [9] L. Ryć, J. Badziak, L. Juha, J. Krása, B. Králiková, L. Láska, P. Parys, M. Pfeifer, K. Rohlena, J. Skála, W. Słysz, J. Ullschmied, M. Węgrzecki and J. Wołowski, 2003 Plasma Phys. Control. Fusion 45 1079.

<sup>&</sup>lt;sup>3</sup> EURATOM Association KFKI-Research Inst. for Particle and Nucl. Physics, Budapest, Hungary

### 2.13 Formation of plasma jets and their interaction with ambient media

Tadeusz Pisarczyk
Institute of Plasma Physics and Laser Microfusion
pisaro@ifpilm.waw.pl

Andrzej Kasperczuk, Stefan Borodziuk, Daniel Baran, Hanna Włodarczyk, Joanna Pokorska, and Jan Pietrzak

#### **Abstract**

Investigations of plasma jet formation induced by the cumulative compression of conically shaped thin foils with the use of the first harmonic of the PALS (Prague Asterix Laser System) iodine laser radiation at the energy of about 550 J were performed. The cones made of Al or Au foils with thicknesses of 9  $\mu m$  and 6  $\mu m$ , respectively, had the apex angle of  $90^{\circ}$  and the height of 250  $\mu m$ . To determine space—time distributions of the electron density inside the plasma jet a new version of three frame interferometric system with high resolution CCD cameras was used. The performed experiments have shown that there is possibility of the cumulative plasma jet creation with parameters very promising from the ICF point of view.

#### Summary

In the fast ignition concept, the target is compressed to high density and then additional energy is applied to the target in order to produce a hot spot. This high temperature increase will start a fusion burning wave that propagates inside the fuel. This additional energy is supplied by hot electrons or ions produced by the interaction of an additional high power laser with a solid target. The fast ignition concept can be realized also substitute the electron beam by a high speed jet driven by the same laser used to illuminate the capsule.

Such a new fast ignitor concept with the use only one energy drive has been proposed by Velarde et al. in the paper [1]. In this concept, the jet is produced in a conical target placed inside a guiding cone, by the collision of high velocity matter accelerated inside a conical guide.

To develop this fast ignition method two-dimensional simulations (by Arwen and Heracles codes) are performed by prof. P. Velarde group from Instituto de Fusión Nuclear in Madrid. The first comparison of these simulations with the experimental results, connected with the formation and propagation of jets, has been presented in the paper [2]. Such experiments were begun on the PALS laser facility( Prague Asterix Laser System).

In this paper the next experimental results inspired by the theoretical and numerical analyses are presented. Investigations were performed with the use of the first harmonic of the PALS iodine laser radiation at the energy of about 550 J.

The cones made of Al foil with thicknesses of 9  $\mu$ m had the apex angle of 900 and the height H=250  $\mu$ m. The target construction and the cross-section photograph of an exemplary Al cone are shown in Fig. 1.

One can estimate that the actual thickness of the cone wall is smaller by about 30% than the initial foil thickness. The focal spot radius, RL, was decreased step by step by 50  $\mu$ m from 250  $\mu$ m to 100  $\mu$ m. It allowed us to get different intensities of the laser radiation at the cones lateral surface. Although in our experiment we started from RL=250  $\mu$ m, satisfactory results were obtained just for RL=100  $\mu$ m. So, these results are demonstrated here. The sequences of electron equidensitograms of the cumulatively produced plasma jets are presented in Fig. 2. One can see that after 1 ns the cumulative jet reaches a distance from the foil surface of about 0.7 mm. Taking into consideration the 0.2 mm plasma way inside the cone, the plasma jet velocity at the first nanosecond was estimated to be higher than 0.8x108 cm/s. However, that high plasma velocity lasts for a very short time, decreasing very fast below 0.4x108 cm/s after next 3 ns. The plasma jet is characterized by a relatively high electron density, considerably above 1019 cm-3, with a steep plasma jet front at the initial stage of the jet propagation.

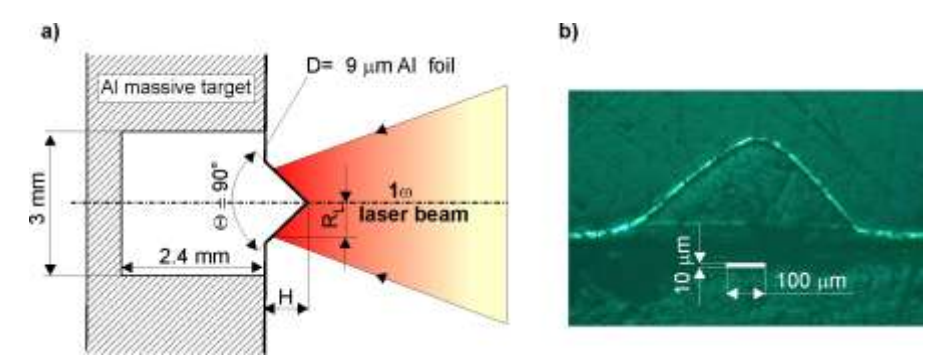


Figure 1. The target construction (a) and the cross-section photograph of the exemplary Al cone (b).

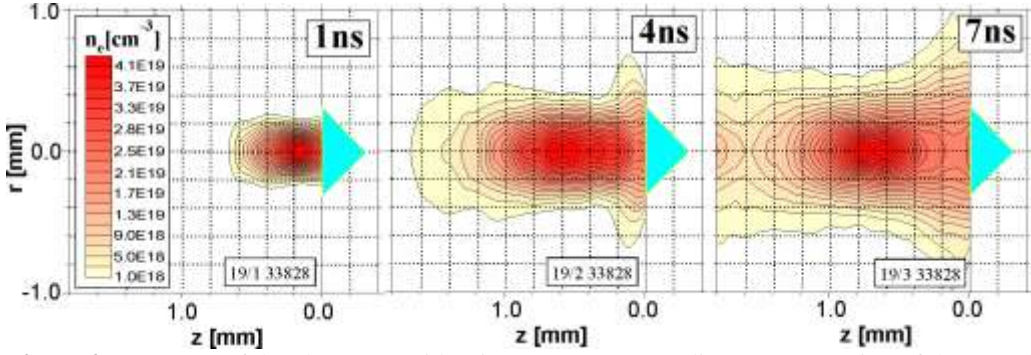


Figure 2. Sequence of the electron equidensitograms corresponding to propagation of the cumulative jet.

Our investigations have shown that using the cumulative effect there is a possibility of creating plasma jets with parameters very interesting from the ICF point of view. The simple method of cone prefabrication by a foil extrusion used by us does not ensure a good quality of the cones. In spite of that the jet velocity observed in our experiment (close to 108 cm/s) seems to be very promising. Of course, the jet parameters achieved in this experiment can be improved. It requires, however, high precision in prefabrication of the cones as well as their highly symmetrical irradiation. Besides, optimization of parameters of the cones (wall thickness, apex angle, material etc.) and of the laser beam (energy, wavelength, intensity distribution etc.) is necessary as well.

Nevertheless, our present investigations made it possible to come to the following crucial conclusions:

- Amongst the two wavelengths used for the cumulative jet generation the shorter one (the third harmonic) appeared to be improper for this purpose. The laser energy transferred into the cone consists of the kinetic energy and of the heating. It turned out that the latter energy plays here a fundamental role.
- Although the theoretical predictions prefer the apex angle of 60° [1] our investigations indicate that the apex angle of 90° might be better.

It is necessary to point out that the reported experiment was purely explorative. The cone quality seems to be crucial for a further progress in the subject. Thus, any subsequent investigations should be performed with the use of professional technology of the cone prefabrication.

#### Collaboration

Association EURATOM – IPP.CR, Prague, Czech Republic PALS Research Center, AS CR, Prague, Czech Republic Instituto de Fusión Nuclear, Madrid, Spain

- [1] P. Velarde, F. Ogando, S. Eliezer, J.M. Martinez-Val, J.M. Perlado, and M. Murakami, LPB 23, 43(2005).
- [2] P. Velarde, M. Gonzalez, C. Garcia-Fernandez, E. Oliva, A. Kasperczuk, T. Pisarczyk, J. Ullschmied, Ch. Stehle, B. Rus, D. Garcia-Senz, E. Bravo and A. Relano: Proc. IFSA 2007, 112 (2008) 042010.